NEUROPHYSIOLOGY

Insulin signaling in AgRP neurons regulates meal size to limit glucose excursions and insulin resistance

Garron T. Dodd[1,2*†‡], Seung Jae Kim[1,2*], Mathieu Méquinion[1,3], Chrysovalantou E. Xirouchaki[1,2], Jens C. Brüning[4,5,6,7], Zane B. Andrews[1,3], Tony Tiganis[1,2,8,9†‡]

The importance of hypothalamic insulin signaling on feeding and glucose metabolism remains unclear. We report that insulin acts on AgRP neurons to acutely decrease meal size and thereby limit postprandial glucose and insulin excursions. The promotion of insulin signaling in AgRP neurons decreased meal size without altering total caloric intake, whereas the genetic ablation of the insulin receptor had the opposite effect. The promotion of insulin signaling also decreased the intake of sucrose-sweetened water or high-fat food over standard chow, without influencing food-seeking and hedonic behaviors. The ability of heightened insulin signaling to override the hedonistic consumption of highly palatable high-fat food attenuated the development of systemic insulin resistance, without affecting body weight. Our findings define an unprecedented mechanism by which insulin acutely influences glucose metabolism. Approaches that enhance insulin signaling in AgRP neurons may provide a means for altering feeding behavior in a nutrient-dense environment to combat the metabolic syndrome.

INTRODUCTION

The obesity epidemic and the associated development of chronic diseases—such as type 2 diabetes, cardiovascular disease, high blood pressure, and cancer—continue to worsen throughout the developed world. In the United States, more than 35% of adults are obese, and it is predicted that by 2030, obesity rates will exceed 50% throughout the majority of the country. Fundamentally, obesity results from a deregulated balance between caloric intake and energy expenditure, processes that are under the control of the brain and the autonomic nervous system.

Homeostatic feeding is coordinated by hypothalamic and brainstem circuitry that normally functions to match feeding with energy expenditure to maintain a relatively stable body weight over time. Within the arcuate nucleus (ARC) of the hypothalamus, agouti-related peptide (AgRP)/neuropeptide Y (NPY)–expressing neurons and proopiomelanocortin (POMC)–expressing neurons represent mutually antagonistic neuronal populations essential for the maintenance of energy homeostasis (*1*, *2*). POMC neurons, when activated, repress feeding and increase energy expenditure through the production of α-melanocyte–stimulating hormone that binds to melanocortin receptors 3/4 in regions such as the paraventricular hypothalamus (*1*, *2*). Conversely, the activation of AgRP/NPY-expressing neurons in the ARC promotes feeding and adaptive behaviors such as foraging that reinforce caloric intake (*3*, *4*). AgRP neurons increase feeding not only through the inhibition of POMC neurons (*5*, *6*) but also independently of the melanocortin circuit (*7*) by projecting to distinct brain regions to regulate feeding in parallel and redundant pathways (*8*). Moreover, both AgRP and NPY can differentially contribute to the temporal dynamics of feeding (*9*–*11*). The importance of AgRP/NPY neurons in feeding is underscored by the overt hypophagia and anorexia associated with the genetic ablation of AgRP neurons (*12*), as opposed to the voracious feeding and heightened food-seeking behavior when AgRP neurons are activated by chemogenetic or optogenetic means (*4*, *7*).

To appropriately orchestrate energy balance, AgRP neurons must integrate diverse signals communicating the energy state of the organism and, in turn, function to adapt feeding to maintain energy balance (*1*). AgRP neurons in the ARC are located close to the median eminence where the blood-brain barrier is fenestrated and are among the first neurons to respond to nutritional cues and metabolic hormones such as leptin and insulin (*1*). Leptin and insulin can activate POMC neurons and promote *Pomc* expression and, at the same time, inhibit AgRP neurons and repress *Agrp* expression (*1*, *2*). Leptin is produced by adipocytes, circulates at levels proportional to body fat content, and is fundamental for body weight control (*13*). Mice that are null for leptin or the leptin receptor (LepR) are hyperphagic and develop morbid obesity and type 2 diabetes (*14*, *15*), whereas mutations of the leptin gene in humans are associated with severe monogenic obesity (*16*).

Leptin signaling in hypothalamic neurons is orchestrated by the protein tyrosine kinase (PTK) Janus-activated kinase 2 (JAK-2) that phosphorylates LepR on Tyr^{1138} to recruit signal transducer and activator of transcription 3 (STAT3); STAT3 is, in turn, tyrosine phosphorylated on Y705 to facilitate its dimerization and translocation to the nucleus where it mediates gene transcription (*13*). Leptin's effects on feeding are largely orchestrated by STAT3, as mutation of Tyr^{1138} on LepR or deletion of STAT3 in LepR-expressing neurons promotes hyperphagia and weight gain (*13*). Insulin is produced by pancreatic β cells in response to postprandial increases in blood glucose. Beyond its well-established glucoregulatory role in peripheral

[1]Metabolism, Diabetes and Obesity Program, Monash Biomedicine Discovery Institute, Monash University, Clayton, VIC 3800, Australia. [2]Department of Biochemistry and Molecular Biology, Monash University, Clayton, VIC 3800, Australia. [3]Department of Physiology, Monash University, VIC 3800, Australia. [4]Max Planck Institute for Metabolism Research, Department of Neuronal Control of Metabolism, Gleueler Str. 50, 50931 Cologne, Germany. [5]Center for Endocrinology, Diabetes, and Preventive Medicine (CEDP), University Hospital Cologne, Kerpener Str. 26, 50924 Cologne, Germany. [6]Excellence Cluster on Cellular Stress Responses in Aging Associated Diseases (CECAD) and Center of Molecular Medicine Cologne (CMMC), University of Cologne, Joseph-Stelzmann-Str. 26, 50931 Cologne, Germany. [7]National Center for Diabetes Research (DZD), Ingolstädter Land Str. 1, 85764 Neuherberg, Germany. [8]Monash Metabolic Phenotyping Facility, Monash University, VIC, Australia. [9]Peter MacCallum Cancer Centre, Melbourne, VIC 3000, Australia.
*These authors contributed equally to this work.
†Corresponding author. Email: garron.dodd@unimelb.edu.au (G.T.D.); tony.tiganis@monash.edu (T.T.)
‡Present address: Department of Anatomy and Physiology, Faculty of Medicine, Dentistry and Health Sciences, University of Melbourne, Melbourne, VIC 3010, Australia.

tissues, insulin also acts in the central nervous system (CNS) to regulate energy expenditure and glucose metabolism through sympathetic and parasympathetic efferent pathways (*1*). Insulin signals via the insulin receptor (IR) PTK and the phosphatidylinositol 3-kinase (PI3K)/protein kinase AKT pathway to mediate its effects on metabolism and energy balance. Early studies established that the intracerebroventricular administration of insulin could repress food intake in rats (*17*) and baboons (*18*), whereas more recent studies have shown that intranasal-administered insulin represses food intake in humans (*19*, *20*). However, the extent to which insulin represses food intake is contentious (*21*, *22*). Moreover, although IR deletion throughout the CNS promotes hyperphagia and obesity (*23*), the specific deletion of the IR in POMC or AgRP neurons in the hypothalamus has no effect on total diurnal food intake (*24*), suggesting that unlike leptin, the anorexic effect of insulin may not involve POMC or AgRP neurons. However, recent studies suggest that such "loss-of-function" approaches can be confounded by the engagement of compensatory mechanisms (*15*).

Here, we have taken advantage of mice that are deficient in the IR tyrosine phosphatase TCPTP (encoded by *Ptpn2*) or the JAK-2 tyrosine phosphatase PTP1B (encoded by *Ptpn1*) in POMC versus AgRP neurons (*22*, *25*–*29*) to explore the impact of enhanced insulin versus leptin signaling on feeding. We report that enhancing the endogenous response to insulin in AgRP but not POMC neurons alters the microstructure of feeding and specifically decreases meal size without influencing total diurnal caloric intake. We demonstrate that the ability of insulin to alter feeding behavior serves to prevent excessive postprandial glucose excursions to attenuate the development of insulin resistance. On the other hand, we demonstrate that enhancing endogenous leptin signaling in AgRP neurons represses total caloric intake without affecting meal size. Our findings define the importance of insulin signaling in AgRP neurons in the coordination of feeding behavior to prevent postprandial hyperglycemia and insulin resistance.

RESULTS

Insulin signaling in AgRP but not POMC neurons affects feeding behavior

We have shown previously that TCPTP inactivates the IR in hypothalamic AgRP and POMC neurons to reduce insulin but not leptin signaling (*22*, *27*, *30*). TCPTP deletion in AgRP neurons enhances both feeding- and insulin-induced PI3K/AKT signaling to inhibit AgRP neurons and the expression of *Agrp* and *Npy* (*27*). Similarly, TCPTP deletion in POMC neurons enhances insulin-induced PI3K/AKT signaling to activate POMC neurons and the expression of *Pomc* to promote melanocortin signaling (*22*, *30*). Accordingly, to determine the extent to which an enhanced response to endogenous insulin might affect feeding, we deleted TCPTP in AgRP or POMC neurons. To this end, we crossed *Ptpn2*$^{fl/fl}$ (C57BL/6) mice with *Agrp-Ires*-Cre (C57BL/6) transgenic mice to excise *Ptpn2* in AgRP/NPY-expressing neurons (*Agrp-Ires*-Cre;*Ptpn2*$^{fl/fl}$: AgRP-TC) in the ARC or *Pomc*-Cre transgenic mice to excise *Ptpn2* in POMC neurons (*Pomc*-Cre;*Ptpn2*$^{fl/fl}$: POMC-TC) and assessed diurnal feeding in male mice using BioDAQ E2 feeding cages. Studies were undertaken in 10-week-old chow-fed mice before any overt effects on body weight and adiposity (Fig. 1A and fig. S1, A to C), otherwise associated with the induction of BAT (brown adipose tissue) activity and WAT (white adipose tissue) browning and the promotion of energy expenditure in AgRP-TC mice (*27*). Ad libitum fed *Ptpn2*$^{fl/fl}$ control mice exhibited normal feeding behavior characterized by a robust increase in food intake during the first 4 hours of the dark phase. This transitioned into small feeding bouts throughout the rest of the dark phase and negligible food intake during the light phase (7:00 a.m. to 7:00 p.m.) of the diurnal cycle (Fig. 1, B to E). As reported previously (*22*, *27*), AgRP-TC or POMC-TC mice exhibited no differences in 24 hours of cumulative food intake when compared to *Ptpn2*$^{fl/fl}$ control mice (Fig. 1C and fig. S1D). However, feeding behavior was significantly altered in AgRP-TC mice, with attenuated food intake during the first 4 hours of the dark cycle (7:00 to 11:00 p.m.), when C57BL/6 mice normally consume most of the food, and enhanced food intake throughout the rest of the dark phase that persisted into the light phase, when food intake is otherwise minimal (Fig. 1, B, D, and E). During the first 4 hours of the dark cycle, the decrease in feeding in AgRP-TC mice was not attributable to a decrease in the number of feeding bouts but rather in the time spent and amount of food consumed per bout (Fig. 1, F to H); although, as reported previously (*27*), AgRP-TC mice exhibited increased diurnal energy expenditure, they did not exhibit differences in ambulatory activity or respiratory exchange ratio or ambulatory activity during the first 4 hours of the dark cycle when meal sizes were reduced (fig. S1, F to K). By contrast, feeding behavior and meal sizes were not altered in POMC-TC mice (Fig. 1, I and J, and fig. S1E) where enhanced insulin signaling is accompanied by increased POMC neuronal activation (*30*). Therefore, deletion of TCPTP in AgRP neurons affects feeding behavior without affecting total caloric intake in ad libitum chow-fed mice, and these effects are independent of their capacity to antagonize POMC neurons. This is line with previous studies showing that AgRP neurons can affect feeding independent of the melanocortin circuit (*7*).

Feeding is accompanied by increased circulating insulin that enters the CNS (*31*). In 10-week-old C57BL/6 mice consuming a standard chow diet, circulating insulin levels rose from 0.93 ± 0.26 ng/μl 30 min before lights off to 2.58 ± 0.21 ng/μl during the first 30 min of the dark cycle when mice are feeding and thereon declined to 1.56 ± 0.29 ng/μl after 4 hours at which time most of the feeding had occurred and then further declined to 0.72 ± 0.27 ng/μl at the start of the light cycle when feeding bouts had largely ceased or were minimal (fig. S2A). By contrast, leptin levels were not affected by feeding during the dark cycle (fig. S2B). We have shown previously that TCPTP deficiency in AgRP neurons promotes PI3K/AKT signaling in the fed and fasted states and antagonizes the activation of AgRP neurons by ghrelin (*27*). To explore whether altered feeding in AgRP-TC mice might be ascribed to the increased postprandial insulin signaling in AgRP neurons, we crossed AgRP-TC mice onto the *Insr*$^{fl/+}$ (C57BL/6) background (*Agrp-Ires*-Cre;*Ptpn2*$^{fl/fl}$;*Insr*$^{fl/+}$: AgRP-TC-IR$^{fl/+}$) so that total IR levels would be reduced by 50% (*27*). We have shown previously that IR heterozygosity in AgRP neurons corrects the otherwise increased insulin-induced ARC PI3K/AKT signaling in AgRP-TC mice as well as the increased energy expenditure and improved glucose metabolism (*27*, *32*). Accordingly, we determined whether IR heterozygosity might similarly correct the altered feeding behavior in AgRP-TC mice. We found that IR heterozygosity had no effect on body weight or adiposity (Fig. 2A and fig. S3A) but largely, albeit not completely, corrected the altered feeding behavior so that meal sizes were largely indistinguishable from control mice (Fig. 2, B to H). By contrast, IR heterozygosity alone in AgRP neurons (*Agrp-Ires*-Cre; *Insr*$^{fl/+}$: AgRP-IR$^{fl/+}$) had no effect on body

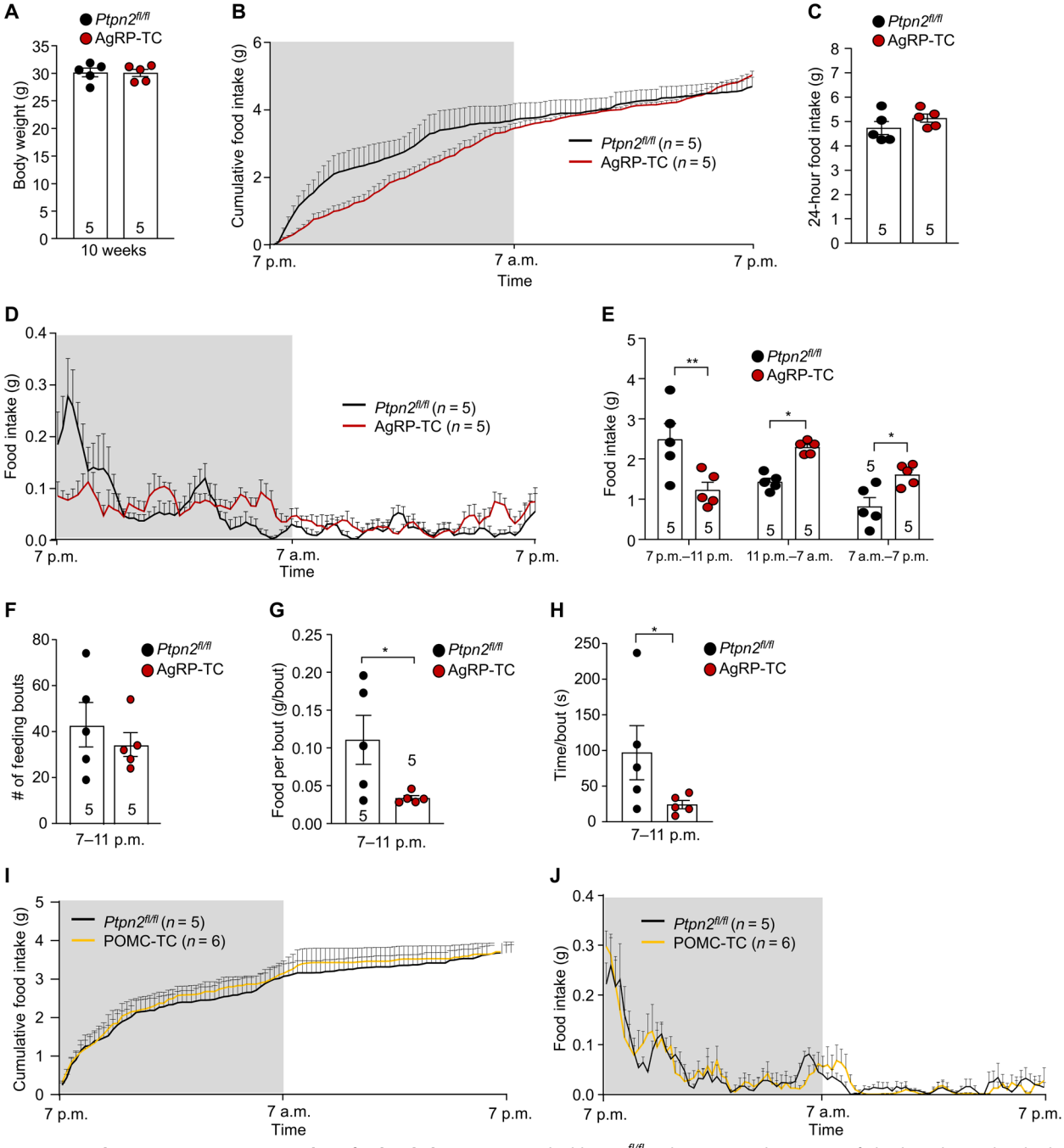

Fig. 1. TCPTP in AgRP but not POMC neurons regulates feeding behavior. Ten-week-old *Ptpn2*$^{fl/fl}$ and AgRP-TC male mice were fed a chow diet, and (**A**) body weights, (**B** and **C**) food intake, and (**D** to **H**) feeding behavior were determined. Ten-week-old *Ptpn2*$^{fl/fl}$ and POMC-TC male mice were fed a chow diet, and (**I**) food intake and (**J**) feeding behavior were determined. Representative and quantified results are shown (means ± SEM) for the indicated number of mice; significance was determined using (E, G, and H) Student's *t* test. **P* < 0.05, ***P* < 0.01.

weight (fig. S3B), adiposity (fig. S3C), feeding behavior (fig. S3, D and E), or cumulative 24-hour food intake (fig. S3, F to J). Therefore, these results causally link the altered feeding behavior in AgRP-TC mice with the promotion of IR signaling.

To provide independent evidence for the ability of insulin signaling in AgRP/NPY neurons to affect feeding behavior, we undertook two experiments. First, we assessed the response to exogenous insulin, administered intraperitoneally just before the start of the dark cycle, on feeding behavior. Although endogenous circulating insulin levels rise rapidly during feeding, we found that the administration of exogenous insulin was able to repress feeding (by repressing bout size) during the first 4 hours of the dark cycle when mice feed (Fig. 3, A to G). However, as seen in AgRP-TC mice that have a heightened response to endogenous insulin, this was compensated for during the rest of the dark cycle and then light cycle so that cumulative 24 hour food intake was unaltered (Fig. 3, B and C).

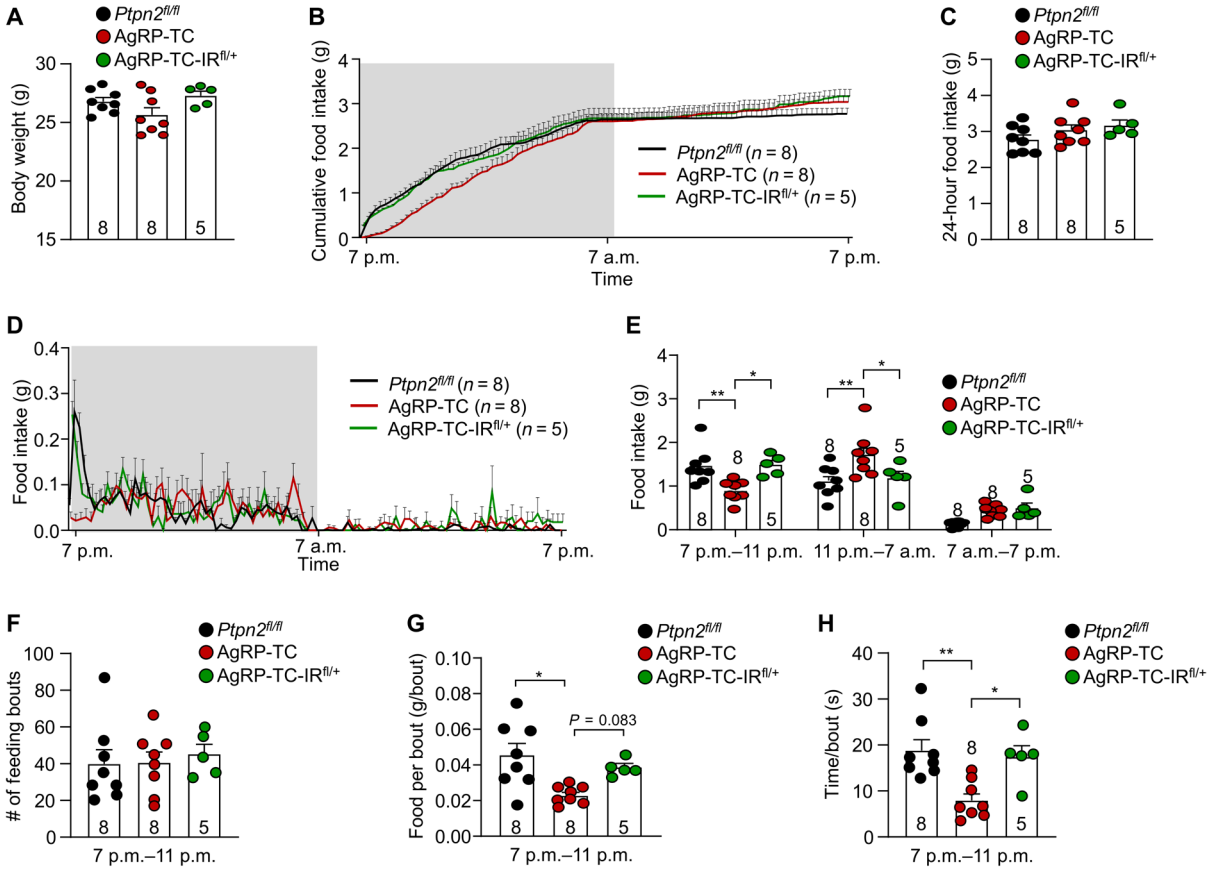

Fig. 2. IR heterozygosity corrects the altered feeding behavior in AgRP-TC mice. Ten-week-old *Ptpn2*$^{fl/fl}$, AgRP-TC, and AgRP-TC-IR$^{fl/+}$ male mice were fed a chow diet, and (**A**) body weights, (**B** and **C**) food intake, and (**D** to **H**) feeding behavior were determined. Representative and quantified results are shown (means ± SEM) for the indicated number of mice; significance was determined using one-way ANOVA. *P < 0.05, **P < 0.01.

Second, we generated mice with a homozygous deletion of IR in AgRP neurons (*Agrp-Ires*-Cre;*Insr*$^{fl/fl}$: AgRP-IR$^{fl/fl}$). We reasoned that if the promotion of insulin signaling in AgRP-TC mice represses feeding during the first 4 hours of the dark cycle, then ablating IR signaling should promote feeding. Consistent with previous studies (*24*), we found that the complete deletion of the IR in AgRP neurons had no effect on body weight (Fig. 3H), adiposity (fig. S3K), or cumulative 24 hour food intake (Fig. 3, I and J). However, whereas food intake was repressed during the first few hours of the dark cycle in AgRP-TC mice, food intake was higher in AgRP-IR$^{fl/fl}$ mice when compared to *Ptpn2*$^{fl/fl}$ controls (Fig. 3, I, K, and L); this was accompanied by a trend for increased feeding per bout without any significant changes in the number of feeding bouts (fig. S3, L and M). Together, these results are consistent with postprandial fluxes in insulin being instrumental in the AgRP neuronal-mediated control of feeding behavior.

Leptin signaling in AgRP neurons reduces caloric intake without affecting feeding behavior

The activity of AgRP neurons is coordinated by varied neuronal, endocrine, nutritional, and environmental cues. It is well established that circulating leptin levels link whole-body adiposity with caloric intake (*1*, *13*). Similar to insulin, leptin also inhibits AgRP neurons and *Agrp*/*Npy* expression and represses feeding (*1*, *13*), whereas the deletion of LepR in AgRP neurons in adult mice promotes hyperphagia, severe obesity, and type 2 diabetes (*15*). To compare the roles of insulin and leptin in feeding, we sought to promote the response to endogenous leptin in AgRP neurons by deleting the tyrosine phosphatase PTP1B (encoded by *Ptpn1*). PTP1B is a key negative regulator of leptin signaling and serves to dephosphorylate JAK-2 and inhibit leptin-induced STAT3 signaling (*25*, *29*). Mice that are deficient for PTP1B in the CNS (*29*), or those in which PTP1B has been deleted in the ARC (*33*), or specifically in AgRP neurons (*28*) are leptin hypersensitive and resistant to diet-induced obesity. To assess how the promotion of endogenous leptin signaling in AgRP/NPY neurons might affect feeding, we crossed *Ptpn1*$^{fl/fl}$ mice with *Agrp*-Ires-Cre transgenic mice to excise *Ptpn1* in AgRP-expressing neurons (*Agrp-Ires*-Cre;*Ptpn1*$^{fl/fl}$: AgRP-1B). PTP1B also negatively regulates insulin signaling (*34*, *35*), and we have shown that elevated hypothalamic PTP1B in diet-induced obesity contributes to the repression of insulin signaling in AgRP neurons (*28*). However, in 8- to 10-week-old chow-fed lean male mice, the deletion of PTP1B in AgRP neurons only marginally promoted PI3K/AKT signaling (~24% above controls) in response to exogenous insulin, as assessed by monitoring for ARC AKT Ser^{473} phosphorylation (p-AKT; Fig. 4A). By comparison, TCPTP deletion in AgRP neurons markedly increased insulin-induced PI3K/AKT signaling (~187% above controls; Fig. 4A). On the other hand, deletion of PTP1B in AgRP neurons significantly

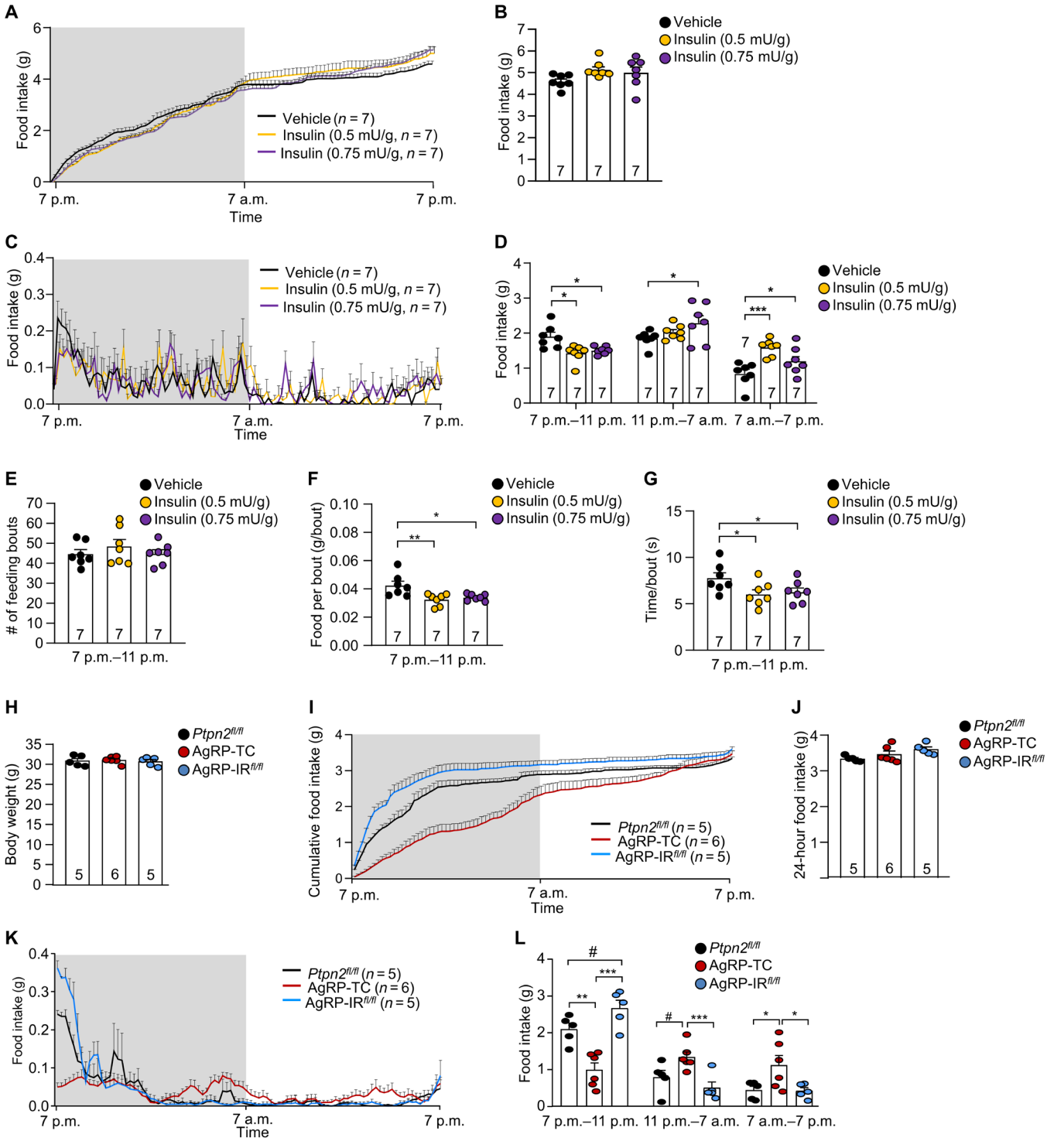

Fig. 3. IR signaling in AgRP neurons regulates feeding behavior. Ten-week-old C57BL/6 mice fed a chow diet were administered either 0.5 or 0.75 mU/g of insulin immediately before the beginning of the dark cycle, and (**A** and **B**) food intake and (**C** to **G**) feeding behavior were determined. Ten-week-old *Ptpn2*$^{fl/fl}$, AgRP-TC, and AgRP-IR$^{fl/fl}$ male mice were fed a chow diet, and (**H**) body weights, (**I** and **J**) food intake, and (**K** and **L**) feeding behavior were determined. Representative and quantified results are shown (means ± SEM) for the indicated number of mice; significance was determined using one-way ANOVA; **P* < 0.05, ***P* < 0.01, ****P* < 0.001. In (L), #*P* < 0.05 represents *Ptpn2*$^{fl/fl}$ versus AgRP-IR$^{fl/fl}$ using Student's *t* test.

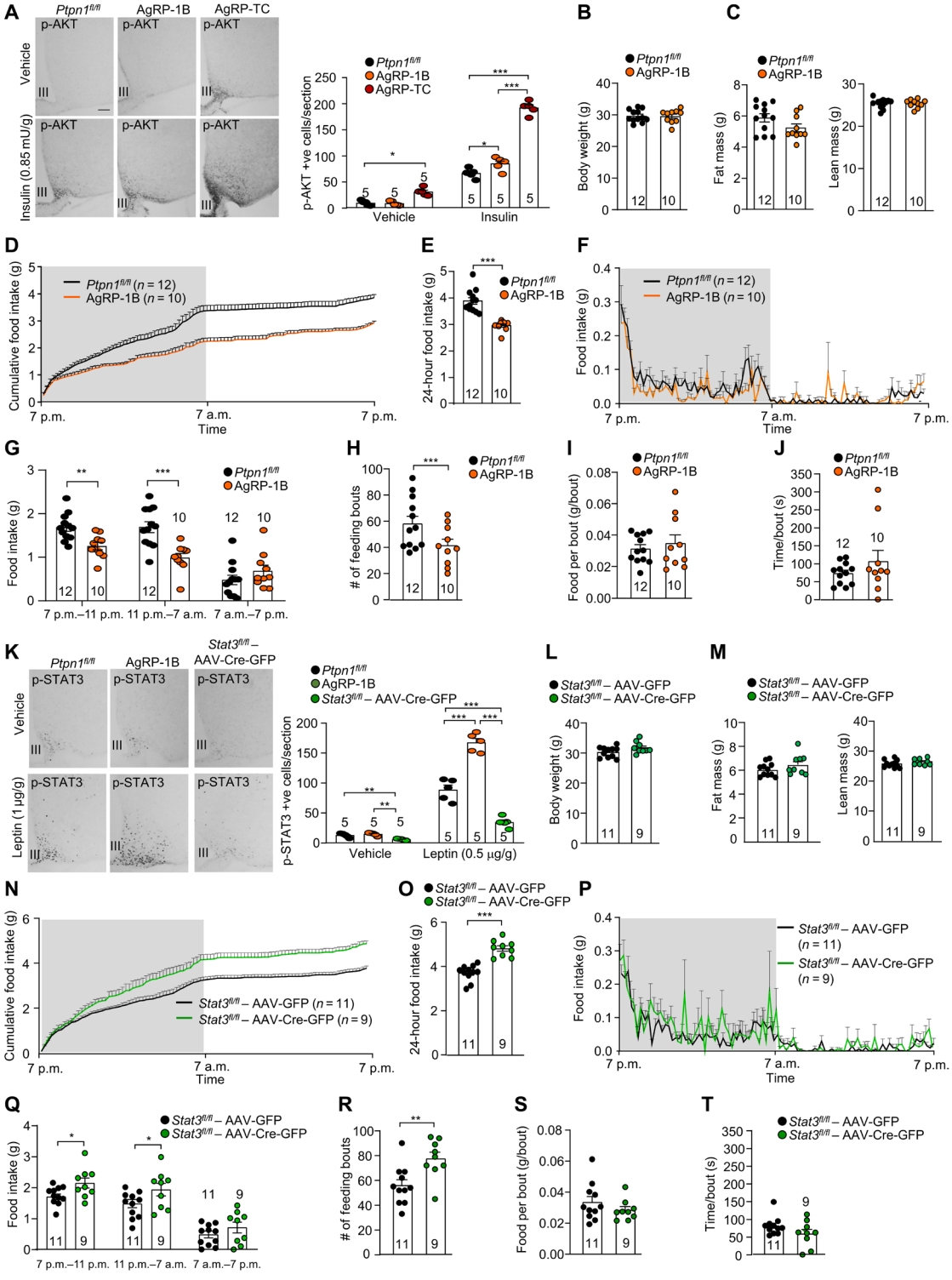

Fig. 4. Leptin signaling regulates caloric intake but not feeding behavior. Eight- to 10-week-old *Ptpn1*$^{fl/fl}$, AgRP-1B, and AgRP-TC male mice were administered vehicle or insulin, and brains were processed for immunohistochemistry monitoring for (**A**) insulin-induced p-AKT. Ten-week-old *Ptpn1*$^{fl/fl}$ and AgRP-1B male mice were fed a chow diet, and (**B**) body weights, (**C**) body composition (EchoMRI), (**D** and **E**) food intake, and (**F** to **J**) feeding behavior were determined. Nine-week-old *Stat3*$^{fl/fl}$ male mice were bilaterally injected with AAV-Cre-GFP into the ARC. Fourteen days after rAVV injection, *Stat3*$^{fl/fl}$ mice versus 10-week-old *Ptpn1*$^{fl/fl}$ and AgRP-1B male mice were administered vehicle or leptin, and brains were processed for immunohistochemistry monitoring for (**K**) leptin-induced p-STAT3. Nine-week-old *Stat3*$^{fl/fl}$ male mice were bilaterally injected with AAV-GFP or AAV-Cre-GFP into the ARC. Fourteen days after rAVV injection, *Stat3*$^{fl/fl}$ mice were fed a chow diet, and (**L**) body weights, (**M**) body composition (EchoMRI), (**N** and **O**) food intake, and (**P** to **T**) feeding behavior were determined. Representative and quantified results are shown (means ± SEM) for the indicated number of mice; significance was determined using (A and K) two-way ANOVA and (E, G, H, O, Q, and R) Student's *t* test. **P* < 0.05, ***P* < 0.01, ****P* < 0.001. Scale bar, 100 μm.

enhanced leptin signaling in the ARC, as assessed by monitoring for ARC STAT3 Y705 phosphorylation (p-STAT3; Fig. 4K). Consistent with our previous studies (*28*), deletion of PTP1B in AgRP neurons had no overt effect on body weight (Fig. 4B) or body composition (Fig. 4C) in 8- to 10-week-old male mice fed a chow diet. As reported previously (*28*), deletion of PTP1B in AgRP neurons significantly repressed diurnal cumulative food intake (Fig. 4, D and E). This was associated with decreased food intake throughout the dark cycle and attributed to a reduction in the number of feeding bouts without any effect on meal size (Fig. 4, F to J). Therefore, the deletion of PTP1B in AgRP neurons and the promotion of leptin signaling repress total food intake but do not affect the size of bouts, as seen when insulin signaling is enhanced.

The effects of leptin on food intake are orchestrated by STAT3 (*36*). To explore further the role of leptin signaling in the coordination of feeding behavior, we assessed the impact of deleting STAT3 in the ARC. To this end, we administered recombinant adeno-associated viruses (rAAVs) expressing green fluorescent protein (GFP) alone (AAV-GFP) or GFP and Cre recombinase (AAV-Cre-GFP) bilaterally into the ARC of 9-week-old *Stat3*$^{fl/fl}$ mice to delete STAT3. We indirectly assessed the efficiency of deletion by monitoring for GFP (fig. S4) and leptin-induced p-STAT3 in the ARC (Fig. 4K). We found that the intra-ARC administration of AAV-Cre-GFP resulted in a marked reduction in basal and leptin-induced p-STAT3 in the ARC. At 14 days after rAAV administration, the deletion of ARC STAT3 was accompanied by a trend for increased body weight ($P = 0.06$; Fig. 4L) but no overt effect on body composition (Fig. 4M). However, the deletion of STAT3 significantly enhanced diurnal food intake (Fig. 4, N to P). Food intake was significantly enhanced throughout the dark cycle (Fig. 4Q); this was accompanied by increased feeding bouts (Fig. 4R) without any effect on meal size (Fig. 4, S and T). Together, our findings affirm that changes in endogenous leptin signaling in ARC neurons affect total food intake without changing feeding behavior. Moreover, our results show that insulin and leptin signaling in AgRP neurons may have nonoverlapping functions in the coordination of diurnal feeding.

Insulin signaling in AgRP neurons does not regulate stereotypical hunger behaviors

AgRP neurons have projection fields that extend throughout the brain (*8*, *37*, *38*). The extensive connectivity affords AgRP neurons the ability to influence not only feeding but also varied hunger-related behaviors, including foraging, anxiety, and repetitive-like behaviors associated with food seeking (*3*, *4*). To determine whether the promotion of insulin signaling and the alterations in feeding behavior associated with the deletion of TCPTP in AgRP neurons might also affect such stereotypical hunger behaviors, we subjected *Ptpn2*$^{fl/fl}$, AgRP-TC, and AgRP-TC-IR$^{fl/+}$ mice to various behavioral tests. These included the elevated plus maze test, a baited open-field test, and marble-burying tests to assess anxiety, exploratory/food seeking, and repetitive-like behaviors. The elevated plus maze test consists of open and closed arms and assesses aversion to open spaces (Fig. 5A), a measure of anxiety. Mice were placed into the elevated plus maze in either the fed (4 hours after lights off) or fasted state (overnight fast). Irrespective of nutritional status, TCPTP deficiency in AgRP neurons did not alter the number of entries or time spent in the closed or open arms (Fig. 5, B and C), suggesting that the promotion of insulin signaling associated with TCPTP deletion in AgRP neurons has no impact on unconditioned anxiety. To further explore for potential effects on anxiety-related behaviors, we used a baited open-field test with a peanut butter chip (a highly palatable food) in the center of the open field to specifically assess anxiety-related food-seeking behaviors (Fig. 5D). TCPTP deletion in AgRP neurons did not alter the time spent or the number of entries in the open-field zones (Fig. 5, E and F) or the distance traveled (fig. S5A). TCPTP deficiency also did not alter the latency for approaching the peanut butter chip (fig. S5B) or the amount of peanut butter chip consumed (Fig. 5G). Together, these results indicate that the deletion of TCPTP and promotion of insulin signaling in AgRP neurons alter feeding behavior without promoting anxiety or repressing food seeking. To determine whether TCPTP deficiency in AgRP neurons and promotion of insulin signaling may affect goal-orientated repetitive behaviors, we subjected mice to marble-burying tests (Fig. 5H). As nutritional status has been shown to affect such repetitive behaviors, marble burying was assessed in both the fed (4 hours after lights off) and fasted (overnight fast) states (*3*). Dietrich *et al.* (*3*) have shown that the chemogenetic activation of AgRP neurons increases repetitive behaviors, as assessed in marble-burying tests. By contrast, we found that deletion of TCPTP and promotion of insulin signaling, which we have shown previously inhibits AgRP neurons (*27*), did not alter marble burying in either the fed or fasted state (Fig. 5, H and I). Therefore, these findings suggest that the inhibition of AgRP neurons by endogenous insulin signaling does not influence stereotypical behavioral responses beyond feeding.

Insulin signaling in AgRP neurons does not affect reward behaviors

Beyond influencing stereotypical hunger-related behaviors, AgRP neurons also have a role in modulating dopaminergic signaling and therefore reward behaviors (*38*–*40*). To determine whether TCPTP deletion and the promotion of insulin signaling in AgRP neurons may affect reward pathways, we first determined whether AgRP-TC mice might exhibit differences in the preference for saccharin-sweetened water, a potent reward stimulus in wild-type C57BL/6 mice, and whether this might be corrected in AgRP-TC-IR$^{fl/+}$ mice (Fig. 6A). We found that TCPTP deletion had no effect on the overt preference that mice showed for saccharin-sweetened water (Fig. 6, B and C, and fig. S6, A and B). To further assess whether TCPTP deletion in AgRP neurons may affect reward pathways, we subjected *Ptpn2*$^{fl/fl}$, AgRP-TC, and AgRP-TC-IR$^{fl/+}$mice to a conditioned place preference test (Fig. 6, D and E). Mice were placed in a conditioning apparatus for 20 min/day for 10 days. The conditioning apparatus had two distinct zones, with either a chow pellet or a highly palatable peanut butter chip, separated by a neutral zone. On the day of the experiment, mice were placed into the neutral middle portion on the apparatus with no added food in either zone, and movements were recorded. As expected, *Ptpn2*$^{fl/fl}$ control mice showed a clear preference for the zone that they associated with the peanut butter chip (Fig. 6E). This preference was not affected by the deletion of TCPTP in AgRP neurons (Fig. 6E). Last, we determined whether the deletion of TCPTP in AgRP neurons might affect the willingness of mice to work for a food reward (Fig. 6, F to H). To this end, we assessed the motivation of *Ptpn2*$^{fl/fl}$ versus AgRP-TC mice for sucrose rewards by subjecting mice fed with a chow diet or a high-fat diet to nose-poke operant conditioning paradigms where the number of pokes required to receive a sucrose pellet reward was progressively increased. There were no genotype differences observed in the rate of food reward acquisition (Fig. 6, F to H, and fig. S7, A

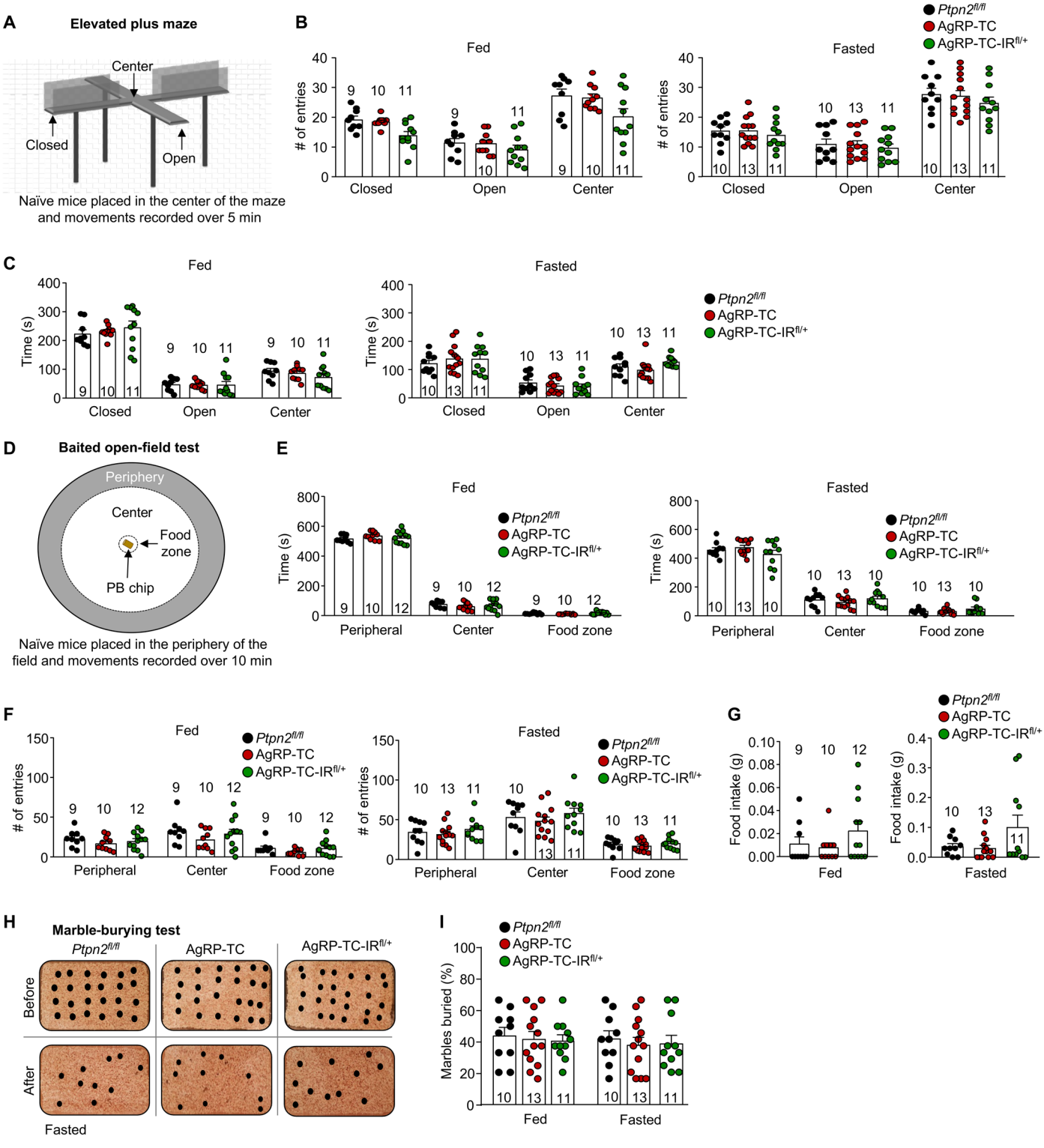

Fig. 5. IR signaling in AgRP neurons does not regulate stereotypic feeding behaviors. (**A**) Ten- to 14-week-old male *Ptpn2*$^{fl/fl}$, AgRP-TC, and AgRP-TC-IR$^{fl/+}$ male mice were subjected to elevated plus maze test to assess anxiety-like behavior in both fed and fasted states, and (**B**) the number of entries and (**C**) the time spent in different parts of the maze were determined. To assess effects on anxiety-related food-seeking behaviors, (**D**) 10- to 14-week-old male *Ptpn2*$^{fl/fl}$, AgRP-TC, and AgRP-TC-IR$^{fl/+}$ male mice were subjected to baited open-field tests in both fed and fasted states, and (**E**) time spent in the different parts of the open field, (**F**) the number of entries, and (**G**) food intake were determined. To measure repetitive behaviors, (**H**) 10-week-old male *Ptpn2*$^{fl/fl}$, AgRP-TC, and AgRP-TC-IR$^{fl/+}$ mice were placed in a cage containing 24 marbles uniformly dispatched, and the (**I**) percentage of marbles buried within 30 min was determined. Representative and quantified results are shown (means ± SEM) for the indicated number of mice. PB, peanut butter.

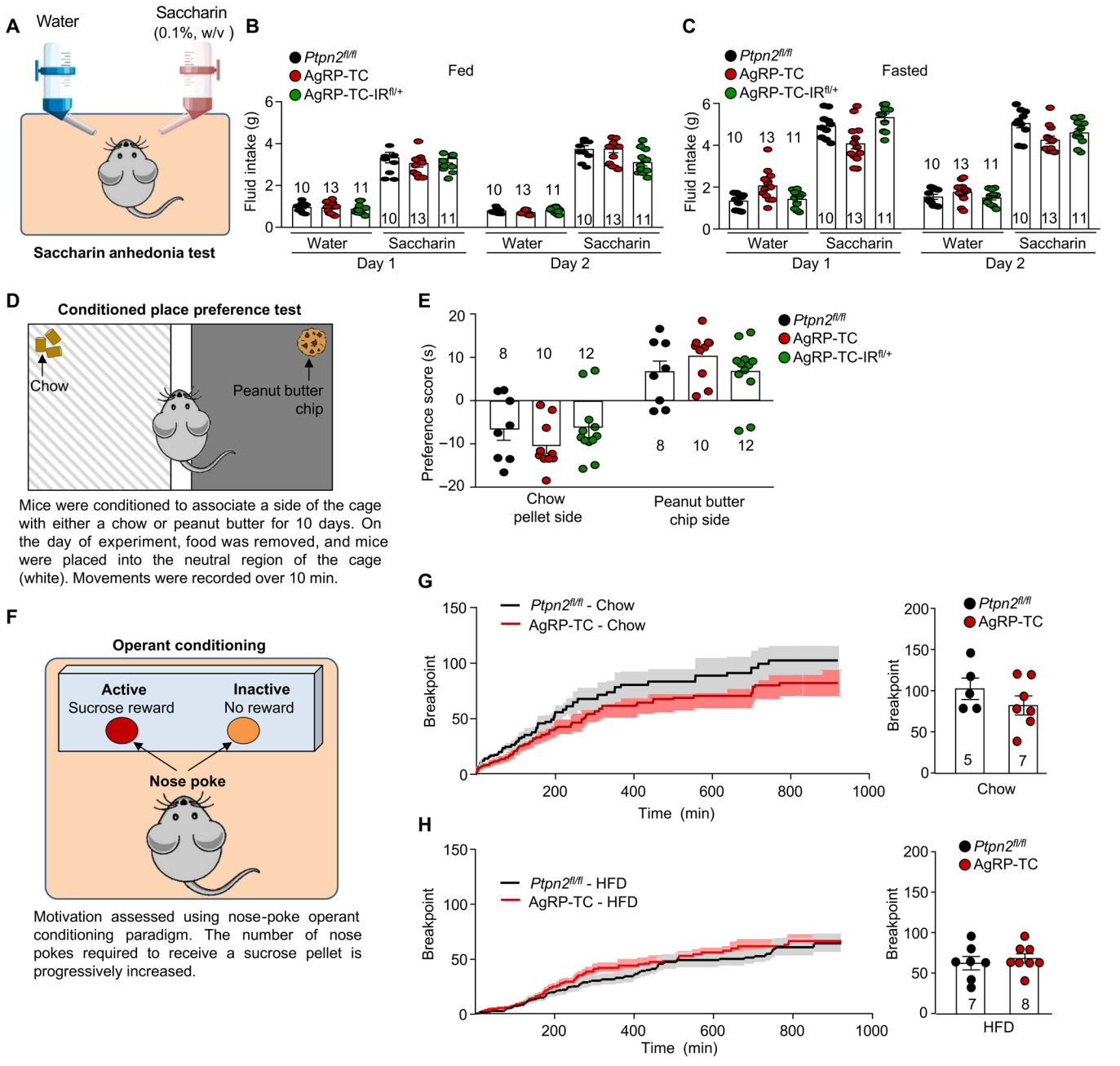

Fig. 6. IR signaling in AgRP neurons does not regulate reward behaviors. To measure reward behaviors, mice were subjected to (**A** to **C**) a saccharin preference test, (**D** and **E**) a conditioned place preference test, or (**F** to **H**) a nose-poke operant conditioning paradigm. (A to C) Twelve-week-old male *Ptpn2*$^{fl/fl}$, AgRP-TC, and AgRP-TC-IR$^{fl/+}$ mice were subjected to saccharin preference tests, and fluid intake in either (B) fed or (C) fasted state was determined. (D and E) Ten- to 14-week-old male *Ptpn2*$^{fl/fl}$, AgRP-TC, and AgRP-TC-IR$^{fl/+}$ mice were associated with the side of the conditioning apparatus with either chow or peanut butter chip for 10 days. On day 10, food was removed, and mice were placed into the neutral region (white box). (D) Schematic of the conditioned place preference test, and (E) time spent in each quadrant of the apparatus was determined. (F to H) Twelve-week-old male *Ptpn2*$^{fl/fl}$ and AgRP-TC mice were subjected to a PR nose-poke operant conditioning paradigm. Mice were fed a chow diet during the FR and the first PR session and then were fed a high-fat diet (HFD) for 5 days before the second PR session. (F) Schematic of operant conditioning test and the motivation breakpoint (the ratio at which mice stop nose poking to receive a sucrose reward) in mice fed with (G) chow or (H) high-fat diet. Representative and quantified results are shown (means ± SEM) for the indicated number of mice.

to F). As an index of motivation, we determined the point at which mice stopped nose poking for rewards. There were no significant differences in the motivation breakpoints between genotypes for mice on the chow versus high-fat diets, indicating that deletion of TCPTP in AgRP neurons does not influence the motivation for sucrose pellets (Fig. 6, F to H). Therefore, our findings demonstrate that the promotion of insulin signaling in AgRP neurons does not affect the dopamine-dependent reward system and that the altered feeding behavior in AgRP-TC mice cannot be ascribed to changes in reward-related behaviors.

Insulin signaling in AgRP neurons diminishes the consumption of palatable food

Although palatability can drive feeding independently of AgRP neurons (*41*), we nonetheless determined whether the promotion of insulin signaling and inhibition of AgRP neurons might repress the consumption of highly palatable high-fat food. To assess this, we provided 10-week-old male *Ptpn2*$^{fl/fl}$ versus AgRP-TC mice fed with a chow diet at baseline with a choice of either chow or high-fat diet (23.5% fat; 46% energy from fat) for 5 days, and the total food consumed and the preference for chow versus high-fat diets were recorded (Fig. 7, A and B). At baseline, ad libitum chow-fed AgRP-TC mice exhibited no differences in body weight (fig. S8A) or body composition when compared to *Ptpn2*$^{fl/fl}$ controls (fig. S8B). When afforded access to both chow and high-fat diets, *Ptpn2*$^{fl/fl}$ control mice showed an immediate and robust preference for the high-fat diet (91.72 ± 5.05% calories/day over 5 days) so that negligible chow diet (8.28 ± 5.05% calories/day over 5 days) was consumed, and this persisted for the subsequent 5 days (Fig. 7, B to E). Despite the almost exclusive consumption of high-fat diet, *Ptpn2*$^{fl/fl}$ control mice did not exhibit any significant difference in total calories consumed per day (Fig. 7C). Although AgRP-TC exhibited an initial preference for the high-fat diet (day 0; Fig. 7B and fig. S8C), consistent with the unaltered hedonic/reward-based responses described earlier (Fig. 6), the overt overall switch from chow to high-fat diet was attenuated in AgRP-TC mice. AgRP-TC mice consumed lower amounts of high-fat diet (63.59 ± 5.70% calories/day over 5 days) when compared to *Ptpn2*$^{fl/fl}$ controls ($P = 0.0001$; Fig. 7, D and E) with some 30 to 40% of their caloric intake being from chow diet; total caloric intake (Fig. 7, D and E), body weight, and body composition were not affected (fig. S8, A and B). These results indicate that heightened insulin signaling in AgRP neurons attenuates the consumption of highly palatable food, without influencing total caloric intake.

Insulin signaling in AgRP neurons attenuates the acute development of insulin resistance

Our studies point toward postprandial fluxes in insulin being instrumental in the AgRP neuronal–mediated control of feeding behavior, limiting the size of meals without affecting total diurnal food intake and suppressing the consumption of highly palatable high-fat food over standard chow. An expected outcome of such altered feeding behaviors might be that feeding-induced glucose and insulin excursions would be decreased and that, in the longer term, this would attenuate the development of systemic insulin resistance. Consistent with this, we found that blood glucose and plasma insulin levels in chow-fed *Ptpn2*$^{fl/fl}$ control mice were elevated after feeding (at 11:00 p.m. when mice were satiated), when compared to levels (at 6:00 p.m.) before the commencement of feeding at lights off (Fig. 8, A and B). By contrast, feeding-induced increases in blood glucose and plasma insulin levels were decreased in chow-fed AgRP-TC mice, but this was corrected in AgRP-TC-IR$^{fl/+}$ mice that were also heterozygous for the IR in AgRP neurons (Fig. 8, A and B), which we have shown is sufficient to correct the increased ARC insulin-induced PI3K/AKT signaling in AgRP-TC mice (*27*). Therefore, the promotion of insulin signaling in AgRP neurons is associated with decreased excursions in circulating blood glucose and insulin levels after feeding.

The acute exposure to a high-fat diet promotes whole-body insulin resistance and dysfunctional glucose metabolism within 3 days of high-fat feeding (*42*). Therefore, to determine whether the heightened insulin signaling in AgRP-TC mice and the consequent effects on meal size and diet preference and the resultant diminished excursions in blood glucose and plasma insulin levels might protect mice from the acute onset of hyperglycemia and insulin resistance, we assessed metabolic health in chow-fed *Ptpn2*$^{fl/fl}$ versus AgRP-TC mice that were afforded access to both the chow and the high-fat diets. To monitor for changes in glucose metabolism, we measured blood glucose and plasma insulin levels in ad libitum fed mice during the day (at 1:00 p.m.) and determined the HOMA-IR (homeostatic model assessment of insulin resistance) index as a measure of whole-body insulin resistance (*43*). This was undertaken before (day 1 of chow-only diet) exposing mice to the high-fat diet and after 5 days of exposure to both chow and high-fat diets (Fig. 8C). Before exposure to high-fat diet, blood glucose, plasma insulin, and the HOMA-IR were not significantly different between *Ptpn2*$^{fl/fl}$ and AgRP-TC mice (Fig. 8, D to F). After 5 days of exposure, *Ptpn2*$^{fl/fl}$ control mice that shifted almost entirely to the consumption of the high-fat diet (Fig. 7) exhibited significantly elevated blood glucose and plasma insulin levels and a significantly increased HOMA-IR index in keeping with the development of systemic insulin resistance (Fig. 8, D to F). Although moderately elevated relative to those in chow-fed controls, blood glucose and plasma insulin levels and the HOMA-IR index were significantly reduced in AgRP-TC mice when compared to *Ptpn2*$^{fl/fl}$ controls after 5 days of exposure to the high-fat diet (Fig. 8F). Together, these results suggest that the promotion of insulin signaling in AgRP neurons represses the acute onset of insulin resistance that is otherwise associated with the innate choice of a highly palatable high-fat diet as the main calorie source.

Our studies indicate that the ability of insulin signaling in AgRP neurons to decrease meal size and the consumption of high-fat food over standard chow diet may be to prevent excessive postprandial glucose excursions to maintain glucose homeostasis and prevent hyperglycemia and the ensuing development of systemic insulin resistance. Accordingly, we reasoned that the deletion of TCPTP in AgRP neurons in chow-fed mice should also repress the intake of carbohydrates in drinking water to prevent exacerbated glucose fluxes during feeding. When chow-fed mice were afforded access to both unsweetened drinking water and sucrose-sweetened drinking water, AgRP-TC mice drank less of the sucrose-sweetened water and more of the unsweetened water during the first 4 hours of feeding (Fig. 9, A to C, and fig. S9, A to C) when plasma insulin levels are highest (fig. S2A); after the peak of feeding and for the remainder of the dark and light cycles, both *Ptpn2*$^{fl/fl}$ controls and AgRP-TC mice showed a preference for sucrose-sweetened drinking consistent with an unaltered hedonic drive (Fig. 9, B and C). The total diurnal fluid intake was the same between *Ptpn2*$^{fl/fl}$ controls and AgRP-TC mice (fig. S9D). Although the homeostatic control of drinking does not involve AgRP neurons, the activation of AgRP neurons can elicit a preference for sweetness (*44*). Therefore, we also determined whether AgRP-TC mice might exhibit a diminished preference for saccharin-sweetened water, which is devoid of nutritional value, during the first 4 hours of the dark cycle (Fig. 9D). No differences were evident between AgRP-TC and *Ptpn2*$^{fl/fl}$ mice when afforded access to unsweetened drinking water versus saccharin-sweetened water, with both groups exhibiting an overt preference for saccharin-sweetened water (Fig. 9, D to F, and fig. S9, E to H). These findings preclude the repressed intake of sucrose-sweetened water in AgRP-TC mice during the peak of feeding being attributable to the inhibition of AgRP neurons and an aversion to sweetness. Instead, these findings

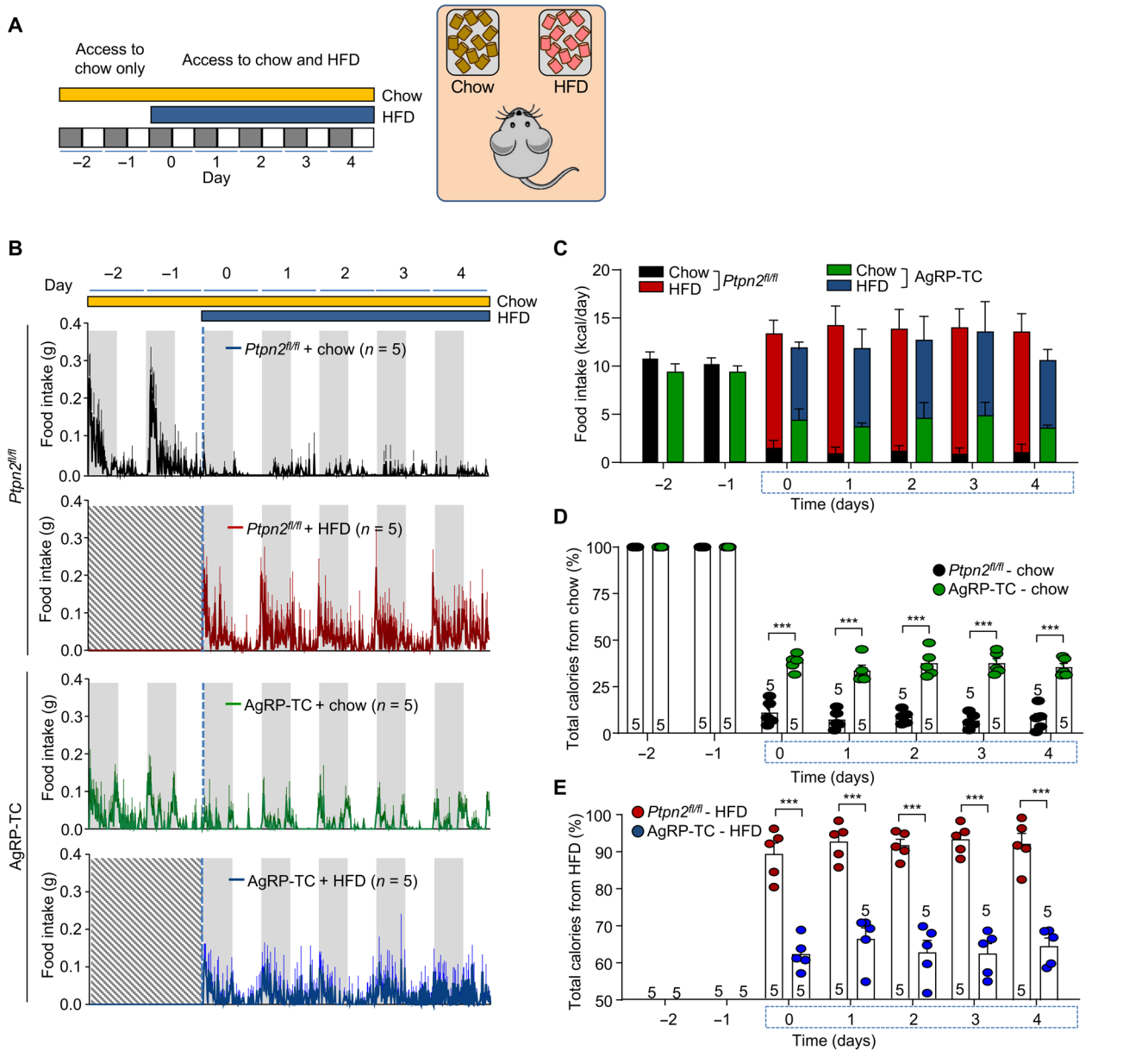

Fig. 7. TCPTP deletion in AgRP neurons attenuates the consumption of high-fat diet. (**A**) Schematic of high-fat diet preference paradigm. Ten-week-old chow-fed *Ptpn2*$^{fl/fl}$ or AgRP-TC mice were exposed to both chow and high-fat diet for 5 days, and (**B**) feeding behavior and (**C** to **E**) the composition of food intake were determined. The dashed blue lines represent the opening of the food hopper gates to allow access to high-fat diet. Representative and quantified results are shown (means ± SEM) for the indicated number of mice using (D and E) two-way ANOVA. ***$P < 0.001$.

are consistent with heightened insulin signaling in AgRP neurons providing a homeostatic signal that serves to decrease meal size and prevent excessive postprandial glucose excursions.

Insulin signaling in AgRP neurons overrides compensatory responses to restricted feeding

Mice with limited access to food learn to anticipate scheduled food access and increase consumption when food is available to prevent weight loss. The activation of AgRP neurons by ghrelin is critical for this anticipatory and compensatory behavior (*45*). We have shown previously that TCPTP deletion and the promotion of insulin signaling antagonize the activation of AgRP neurons by ghrelin (*27*). In this study, we demonstrate that insulin signaling in AgRP neurons decreases the size of meals or the consumption of high-fat food or sucrose-sweetened water to prevent excessive glucose and insulin excursions. We therefore asked whether the promotion of insulin signaling in AgRP neurons might be sufficient to override the ghrelin-mediated compensatory behavior and the increased glucose excursions due to increased feeding that might be expected from restricting food access to the first 4 hours of the dark cycle. Notably, we found that enhanced insulin signaling in AgRP-TC mice prevented the adaptation to the 4-hour restricted feeding regime (Fig. 10). *Ptpn2*$^{fl/fl}$ control mice increased their food intake from 1.34 ± 0.17 to 3.81 ± 0.64 g (Fig. 10, B, D, and E) by the third night and maintained a stable

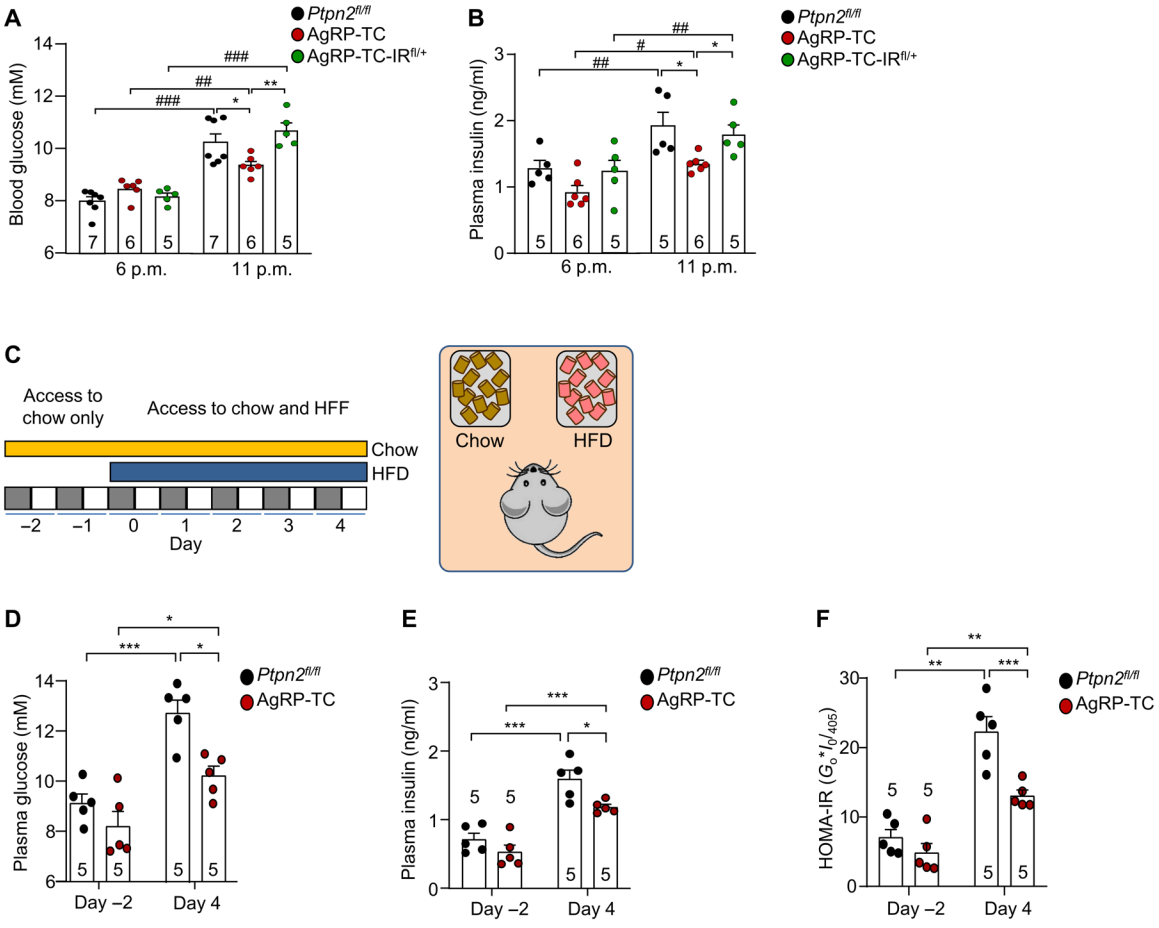

Fig. 8. Insulin signaling in AgRP neurons attenuates the acute development of insulin resistance. Eight-week-old chow-fed *Ptpn2*$^{fl/fl}$, AgRP-TC, and AgRP-TC-IR$^{fl/+}$ male mice were fed a chow diet, and (**A**) blood glucose and (**B**) plasma insulin levels were determined at 6:00 and 11:00 p.m. (**C**) Schematic of high-fat diet preference paradigm. Ten-week-old chow-fed *Ptpn2*$^{fl/fl}$ or AgRP-TC mice were given access to both chow and high-fat diet for 5 days, and (**D**) blood glucose and (**E**) plasma insulin levels were measured (at 2:00 p.m.), and (**F**) HOMA-IRs were calculated on days −2 (chow only) and 4 (5 days of exposure to chow and high-fat diet). Representative and quantified results are shown (means ± SEM) for the indicated number of mice; significance was determined using (A, B, and D to F) two-way ANOVA; **P* < 0.05, ***P* < 0.01, and ****P* < 0.001. In (A) and (B), #*P* < 0.05, ##*P* < 0.01, and ###*P* < 0.001 represent significance determined using Student's *t* test.

body weight over four nights of restricted feeding (Fig. 10F). The increased food intake for *Ptpn2*$^{fl/fl}$ mice was accompanied by an increase in blood glucose (assessed at 11:00 p.m. on the second night). By contrast, AgRP-TC mice did not adjust their feeding (Fig. 10, B, D, and E). Although this resulted as expected in decreased glucose excursions (Fig. 10C), the caloric deficit was also accompanied by markedly decreased body weight and adiposity without change in lean mass (Fig. 10, F and G). The effects on feeding, blood glucose, and body weight were corrected in AgRP-TC-IR$^{fl/+}$ mice (Fig. 10, B to G) consistent with these being attributed to the promotion of insulin signaling. Therefore, the promotion of insulin signaling in AgRP neurons in insulin-hypersensitive AgRP-TC mice can override the compensatory responses to restricted feeding. This not only prevents increased feeding-induced glucose excursions but also additionally facilitates weight loss.

DISCUSSION

The pancreatic hormone insulin, which crosses from the circulation into the brain, was the first hormone to be implicated in the CNS control of body weight (*18*). Subsequently, the identification of leptin as a key adiposity factor regulating energy balance (*14*) largely overshadowed the role of ARC insulin signaling. Moreover, although the IR is particularly abundant in the hypothalamus, its deletion in POMC or AgRP neurons does not affect cumulative food intake or energy expenditure (*24*). This led to the erroneous conclusion that ARC insulin signaling does not have a role in the homeostatic control of energy balance. Our recent studies have challenged this assertion and have shown that insulin signaling in POMC and AgRP neurons is fundamentally important for the homeostatic control of energy expenditure through the coordination of feeding with WAT browning and thermogenesis (*22*, *27*). By taking advantage of genetic approaches that enhance the response to endogenous insulin versus leptin, we now also demonstrate that insulin not only affects feeding behavior and thereby influences glucose metabolism but also that its effects on feeding are distinct from those of leptin.

The reasons for the lack of effects on energy balance when the IR is deleted in POMC or AgRP neurons during embryogenesis (*24*) remain unclear. In part, this may be attributable to compensatory processes arising during embryonic development. Consistent with

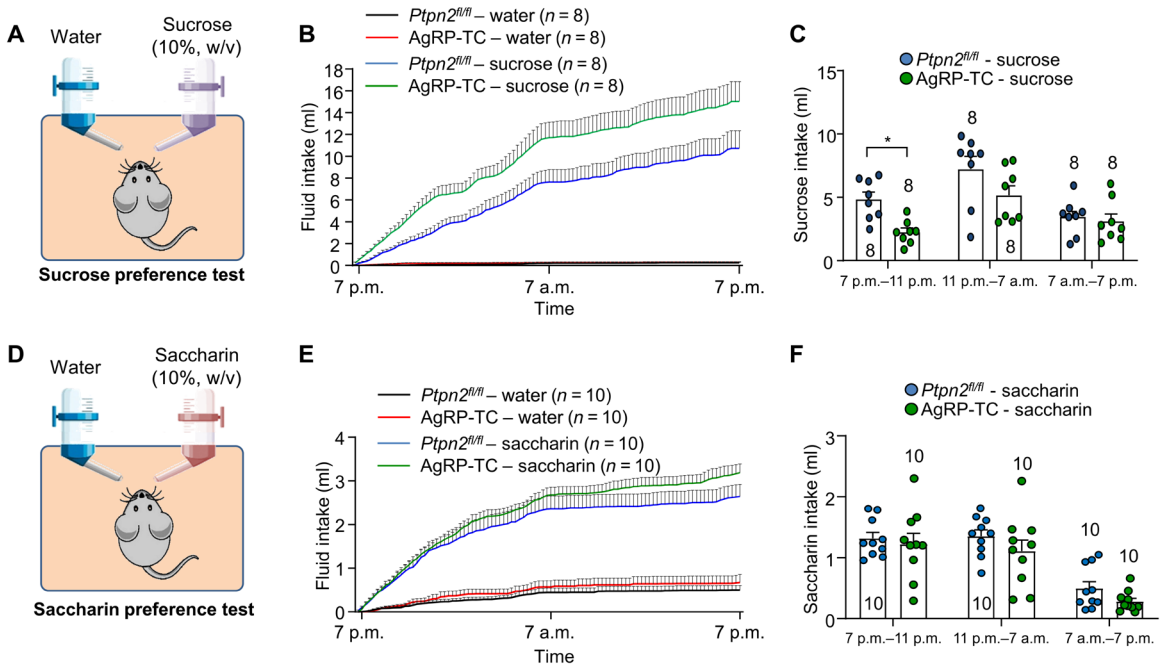

Fig. 9. Insulin signaling in AgRP neurons attenuates the consumption of sucrose- but not saccharin-sweetened water. (**A**) Schematic of sucrose preference test. Eight-week-old chow-fed *Ptpn2*$^{fl/fl}$ or AgRP-TC mice were given access to both water and 10% sucrose solution, and (**B**) fluid intake and (**C**) drinking behavior were determined. (**D**) Schematic of saccharin preference test. Eight-week-old chow-fed *Ptpn2*$^{fl/fl}$ or AgRP-TC mice were given access to both water and 0.1% saccharin solution, and (**E**) fluid intake and (**F**) drinking behavior were determined. Representative and quantified results are shown (means ± SEM) for the indicated number of mice; significance was determined using (C) Student's *t* test. *$P < 0.05$.

this, the Cre/LoxP-mediated deletion of LepR in AgRP neurons has mild effects on feeding and body weight (*46*), whereas the CRISPR-Cas9–mediated ablation of LepR in AgRP neurons in adult mice promotes voracious feeding and obesity similar to that seen in *Ob/Ob* mice (*15*). Alternatively, the effects on energy balance and especially feeding may be nuanced and may have been missed by previous studies. In this study, we demonstrate that insulin signaling in AgRP neurons limits the size of meals, without affecting total diurnal caloric intake. Although, in itself, this does not affect energy balance, we demonstrate that the control of meal size is fundamentally important for limiting postprandial glucose and insulin excursions. Mice with heightened insulin signaling in AgRP neurons consumed less food during the first 4 hours of the dark cycle, when mice otherwise consume most of their food. As a consequence, postprandial glucose and insulin excursions in fed/satiated mice, when glucose and insulin are normally at their highest, were decreased. Notably, when AgRP-TC mice were afforded access to both chow and high-fat diets, they consumed less of the high-fat diet, and this markedly attenuated the development of systemic insulin resistance and hyperglycemia. This was not due to a diminished feeding drive. Moreover, stereotypical hunger responses and reward behaviors were not affected. Instead, we assert that the decreased consumption of otherwise highly palatable high-fat food by AgRP-TC mice might have been attributable to the heightened resultant glucose and insulin excursions, which we speculate would favor the consumption of chow diet to limit glucose spikes in insulin-hypersensitive AgRP-TC mice. Consistent with this, we found that AgRP-TC mice also drank less sucrose-sweetened water during the peak of feeding but exhibited no differences when afforded access to saccharin-sweetened water that has no calorific value. We propose that the capacity for insulin signaling in AgRP neurons to limit meal size and the consumption of meals with a high glycemic index may normally serve to prevent excessive feeding-induced glucose and insulin excursions and provide an important homeostatic feedback mechanism for attenuating the development of hyperglycemia and systemic insulin resistance without compromising total diurnal caloric intake and thereby anabolic growth/survival. The importance of this homeostatic glucomodulatory response is underscored by the capacity of insulin signaling in AgRP-TC mice to even override the increased anticipatory feeding normally associated with timed food restriction that otherwise results in elevated postprandial blood glucose. Our findings are reminiscent of the "glucostatic" theory for the regulation of feeding first proposed in 1953 (*47*), which argues that low blood glucose promotes feeding and high blood glucose promotes meal termination (*47*), as well as early studies in humans showing that a decrease in blood glucose is associated with the initiation of feeding (*48*, *49*). Although the effects of glucose/glycemic index on meal size and food intake in humans is controversial, there are studies that support that carbohydrate ingestion and increased blood glucose levels stimulate short-term satiety to reduce food intake in humans (*50*, *51*). In obesity, where peripheral and hypothalamic insulin resistance pervades, this homeostatic glucostatic mechanism would be abrogated and may contribute to the progressive development of type 2 diabetes.

Although the promotion of insulin signaling limited the size of meals at the peak of feeding, total caloric intake was unaffected as mice compensated by consuming more food at later times. The compensatory neural mechanisms that ensured that total food intake was not affected by TCPTP deficiency and promotion of insulin signaling in AgRP neurons are not clear. It is possible that the

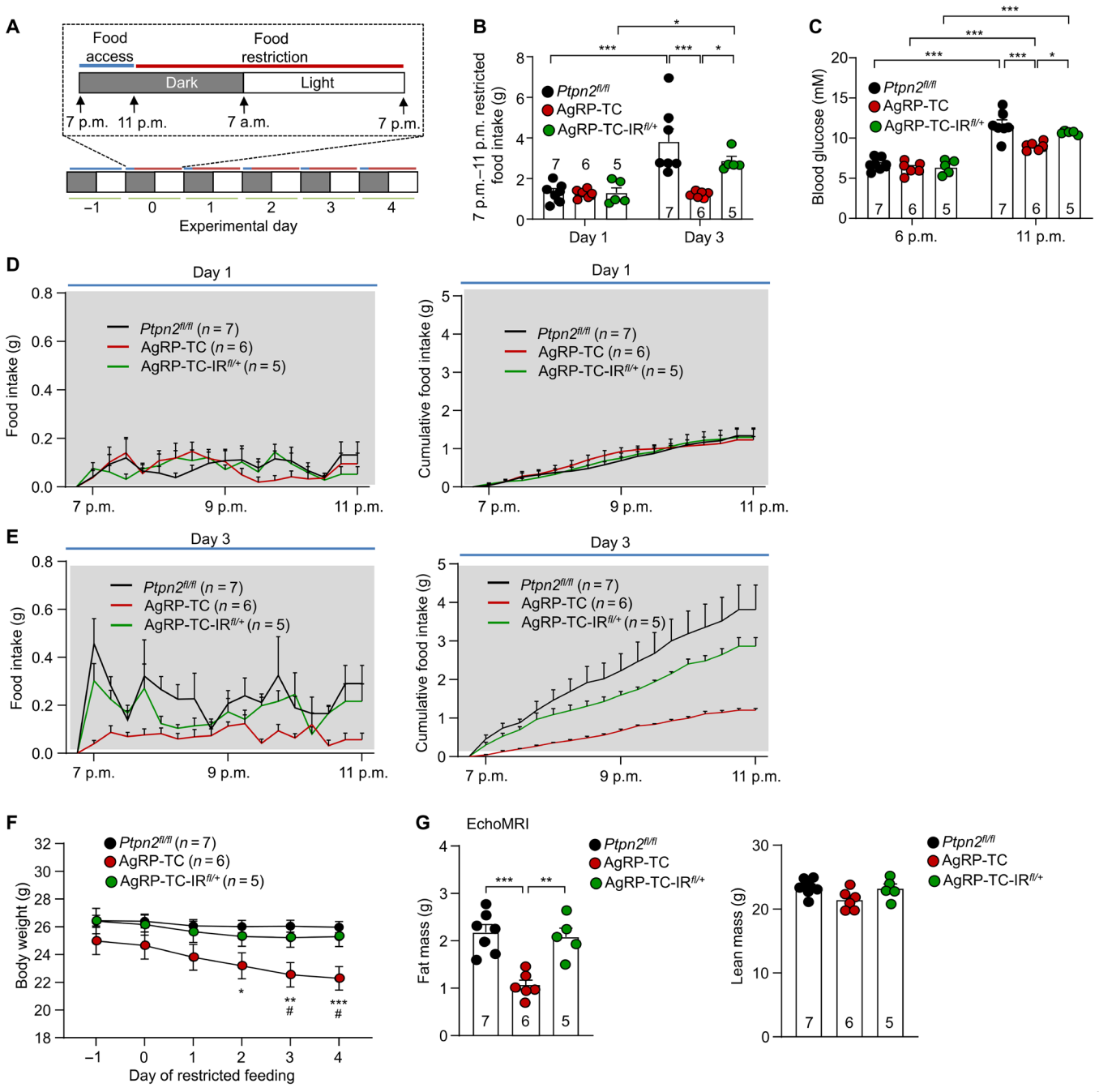

Fig. 10. IR signaling in AgRP neurons overrides compensatory feeding responses to restricted feeding and limits glucose excursions. Ten-week-old *Ptpn2*$^{fl/fl}$, AgRP-TC, and AgRP-IR$^{fl/+}$ male mice were subjected to a restricted feeding paradigm, whereby mice were granted access to food during only the first 4 hours of the diurnal feeding cycle (7:00 p.m. until 11:00 a.m.). (**A**) Schematic of restricted feeding paradigm. (**B** and **D**) Food intake and (**E**) feeding behavior were determined on days 1 and 3 of restricted feeding. (**C**) Blood glucose levels were determined at 6:00 and 11:00 p.m. on day 2 of restricted feeding. (**F**) Daily body weights of *Ptpn2*$^{fl/fl}$ and AgRP-TC male mice throughout the 4 days of restricted feeding. (**G**) Body composition (EchoMRI) following 4 days of restricted feeding. Representative and quantified results are shown (means ± SEM) for the indicated number of mice; significance was determined using (B and C) two-way ANOVA, (F) two-way ANOVA with repeated measures, and (G) one-way ANOVA; **P* < 0.05, ***P* < 0.01, and ****P* < 0.001. In (F) #*P* < 0.05 represents significance determined using Student's *t* test.

deletion of TCPTP in AgRP neurons may facilitate the engagement of hindbrain circuits that regulate meal size/termination and total caloric intake. Satiety signals conveyed by gut-derived hormones, such as glucagon-like peptide 1, act upon vagal sensory fibers that activate caudal hindbrain neurons that directly project to the hypothalamus or, otherwise, indirectly relay signals to the hypothalamus by activating calcitonin gene-related peptide (CGRP)–expressing neurons in the parabrachial nucleus to decrease meal size (*52*, *53*). AgRP neurons can inhibit anorexigenic CGRP-expressing neurons in the parabrachial nucleus, and this can increase meal size, but this

is accompanied by compensatory decreased feeding frequency so that total caloric intake and body weight remain unaltered (*52*, *53*). We speculate that the promotion of insulin signaling and inhibition of AgRP neurons in AgRP-TC mice might accentuate hindbrain satiety signaling to facilitate the activation of CGRP-expressing neurons, so that meal size is initially repressed but compensated for later so that total caloric intake ultimately remains unaltered.

The chemogenetic or optogenetic activation of AgRP neurons can drive stereotypical feeding behaviors such as foraging, as well dopamine reward circuits that increase the rewarding effects of food (*3*, *54*). By contrast, we found that the deletion of TCPTP and the promotion of inhibitory insulin signaling in AgRP neurons did not alter stereotypical feeding behaviors or the rewarding value of food. In particular, AgRP-TC mice showed no differences in conditioned place preference tests or differences in their predilection for sucrose pellets or saccharin-sweetened water. The lack of differences in preference for saccharin-sweetened water also suggests that decreased feeding could not be ascribed to anhedonia, which is consistent with tests showing no differences in anxiety. One possible reason for these findings may be that the duration and/or the relative degree of AgRP neuronal activation after feeding may be vastly different from that associated with chemogenetic/optogenetic approaches manipulating AgRP neuronal activity. Although chemogenetic/optogenetic approaches are powerful tools for establishing potential neuronal functions, they can elicit responses that extend beyond physiological parameters (*55*). However, it may also reflect insulin engaging discreet subsets of AgRP neurons, rather than indiscriminately affecting all AgRP neurons, as would occur with chemogenetic/optogenetic manipulations. Distinct subsets of leptin- versus insulin-responsive POMC neurons exist in the ARC (*56*), and the combined deletion of LepR and IR in POMC neurons yields synergistic outcomes on glucose metabolism (*57*). Our studies have shown that leptin and insulin act on different subsets of POMC neurons to increase the sympathetic outflow to WAT to promote browning and energy expenditure (*22*). Elegant circuit-mapping techniques have shown that different subsets of AgRP neurons exist that project to different regions of the brain to regulate feeding versus glucose metabolism (*8*, *37*). In particular, Betley *et al.* (*8*) reported that several redundant neural circuits originating from distinct AgRP neurons can independently regulate feeding. Although the distribution of IR and LepR in AgRP neurons remains to be determined, it is possible that the IR and LepR may be expressed in different subsets and that this may allow for inhibitory insulin versus leptin signaling to differentially affect meal size versus feeding frequency and thereby glucose homeostasis versus total caloric intake and body weight.

In summary, our studies have defined a previously unidentified homeostatic role for AgRP neuronal insulin signaling in coordinating feeding behavior for the purposes of maintaining glucose homeostasis and preventing the development of insulin resistance. Our findings highlight the capacity for inhibitory leptin versus insulin signaling in AgRP neurons to elicit distinct effects on feeding to independently influence body weight versus glucose homeostasis.

MATERIALS AND METHODS

Mice

Ptpn1$^{fl/fl}$, *Ptpn2*$^{fl/fl}$, *Insr*$^{fl/fl}$, *Agrp*-Ires-Cre;*Ptpn1*$^{fl/fl}$ (AgRP-1B), *Agrp*-Ires-Cre;*Ptpn2*$^{fl/fl}$ (AgRP-TC), *Agrp*-Ires-Cre;*Ptpn2*$^{fl/fl}$;*Insr*$^{fl/+}$ (AgRP-TC-IR$^{fl/+}$), *Agrp*-Ires-Cre;*Insr*$^{fl/fl}$ (AgRP-IR$^{fl/fl}$), *Pomc*-Cre;*Ptpn2*$^{fl/fl}$ (POMC-TC), and *Stat3*$^{fl/fl}$ mice have been described previously (*22*, *27*, *28*, *32*, *58*). To generate *Insr*$^{fl/+}$ and *Agrp*-Ires-Cre;*Insr*$^{fl/+}$ (AgRP-IR$^{fl/+}$) mice, AgRP-IR$^{fl/fl}$ mice were mated with C57BL/6J mice. Mice were maintained on a 12-hour light-dark cycle in a temperature-controlled high-barrier facility with free access to food and water. Mice were fed a standard chow (8.5% fat) or a high-fat diet (23% fat; 45% of total energy from fat; SF04-027, Specialty Feeds) as indicated. Male mice were used in all studies. All mice were on a C57BL/6J background. When necessary, experiments were undertaken under reverse light cycle conditions (lights off, 11:00 a.m.) with the mice acclimatized for 10 to 12 days before any intervention. Experiments were approved by the Monash University School of Biomedical Sciences Animal Ethics Committee.

Food intake experiments

We maintained mice on a 12-hour light-dark cycle from 7:00 p.m. (lights off) to 7:00 a.m. (lights on). Diurnal feeding was assessed using BioDAQ E2 cages (Research Diets, NJ) after a 48-hour acclimation period. Mice were singly housed, and food intake was measured over a 24-hour period and grouped into time bins. BioDAQ feeding cages were fitted with computer-controlled automatic gates to prevent access to feeding hoppers during fasting experiments to allow stress-free intervention without human interaction. For restricted feeding experiments, gates were programmed to open at 7:00 p.m. and close at 11:00 p.m., allowing a 4-hour window for ad libitum food access.

Functional immunohistochemistry

For ARC immunohistochemistry monitoring for STAT3 Y705 phosphorylation (p-STAT3) or AKT S473 phosphorylation (p-AKT), mice were fasted overnight for 16 hours and then injected intraperitoneally with either vehicle, leptin (1 μg/g, i.p.; PeproTech, Israel) or vehicle, or insulin (0.85 mU/g, i.p.; Actrapid, Novo Nordisk, Denmark), respectively. Mice were anesthetized at either 15 min (p-AKT staining) or 45 min (p-STAT3) after injection and perfused transcardially with heparinized saline [1000 U/liter of heparin in 0.9% (w/v) NaCl] followed by 4% (w/v) paraformaldehyde in phosphate buffer (0.1 M, pH 7.4). Brains were postfixed overnight and cryopreserved in 30% (w/v) sucrose in 0.1 M phosphate buffer for 3 days, before freezing on dry ice. Thirty-micrometer sections (120 mm apart) were cut in the coronal plane throughout the entire rostral-caudal extent of the hypothalamus.

For both p-STAT3 and p-AKT immunostaining, we followed previously described procedures in (*33*). Sections were pretreated for 20 min in 0.5% (w/v) NaOH and 0.5% (v/v) H_2O_2 in phosphate-buffered saline, followed by immersion in 0.3% (w/v) glycine for 10 min. Sections were then placed in 0.03% (w/v) SDS for 10 min and placed in 4% (v/v) normal goat serum and 0.4% (w/v) Triton X-100 for 20 min before incubation for 48 hours with anti–p-STAT3 (Y705) antibody (1:500; #9131, Cell Signaling Technology, Beverly, MA) or rabbit anti–p-AKT (Ser^{473}) (1:300; #4060, Cell Signaling Technology, Beverly, MA). p-STAT3– and p-AKT–positive cells were visualized using rabbit immunoglobulin G VECTASTAIN ABC Elite and DAB solution [0.5 mg/ml of 3,30-diaminobenzidine in 0.1% (v/v) H_2O_2]. p-STAT3 and p-AKT immunopositive cells were counted using a bright-field microscope.

Metabolic measurements

Blood glucose levels were determined using an Accu-Chek glucometer (Roche, Germany), and plasma insulin levels were determined

using the rat/mouse insulin ELISA (enzyme-linked immunosorbent assay) (EZRMI-13K, Sigma-Aldrich, St. Louis, MO) or the mouse insulin ELISA (80-INSMS-E01, ALPCO, Salem, NH). Where blood glucose and plasma insulin levels were measured at 6:00 and 11 p.m., food was removed at 3:00 p.m. to achieve a consistent baseline and returned at 6:30 p.m. before lights off at 7:00 p.m. Plasma leptin levels were determined using a mouse leptin ELISA (Merck Millipore, Darmstadt, Germany). The HOMA-IR was calculated using the equation [(glucose × insulin) / 405].

Body composition was assessed using EchoMRI (Echo Medical Systems, Houston, TX). Alternatively, body composition (lean, fat, and bone mineral density) was measured by dual-energy x-ray absorptiometry (Lunar PIXImus2, GE Healthcare, Chicago, IL) and analyzed using PIXImus2 software.

Behavioral tests

For behavioral tests, mice were group-housed in between experiments. The elevated plus maze and modified open-field tests were performed on fed versus fasted mice using different cohorts to negate fear sensitization confounding results. Mice in the fed state were placed in reverse light cycle (lights off, 11:30 a.m.; lights on, 11:30 p.m.) with 10 to 12 days of acclimation before tests being performed between 10:00 and 11:00 a.m. Food was restricted 4 hours before lights off with food returned at lights off to ensure uniform satiety between groups; mice were allowed to feed for 4 hours, and food was removed 1 hour before testing. Mice in the fasted state were housed under normal light cycle (lights off, 8:00 p.m.; lights on, 8:00 a.m.), fasted overnight, and tests were performed between 9:00 and 11:30 a.m. Except for the marble-burying test, all behavioral tests were video-recorded and analyzed using the video-tracking software TopScan (CleverSys Inc., Reston, VA) with the center of the body used as the tracking point in different parts of the apparatus. In between experiments, all apparatus were cleaned with 30% ethanol.

Elevated plus maze

The elevated plus maze was conducted as described previously (*59*). In brief, fed or fasted mice (as described above) were placed in a plus-shaped maze consisting of two closed arms [30 cm (length) by 5 cm (width) by 20 cm (height)] and two open arms [30 cm (length) by 5 cm (width)] raised to 40 cm from the floor through metal legs. The time spent and the entries in the different parts of the apparatus (closed arms, open arms, and center) were measured.

Baited open-field test

The baited open-field test was conducted as described previously (*59*). One week prior, mice were exposed three times randomly to the peanut butter chips (Reese's peanut butter chips, The Hershey Company, Hershey, PA) to prevent neophobia (*59*). The open-field area (Ø 800 mm) was segregated into peripheral and central zones with the peripheral zone defined as 280 mm from the peripheral walls, and the central zone was defined as the area beyond 280 mm from the walls to the center of the arena. At the start of the experiment, a peanut butter chip was placed in the center zone of the open-field arena and fixed to the floor with Blu Tack (Bostik). For quantification, the arena was segregated into a peripheral zone and a central zone. All mice were placed in the open field at the same region against the peripheral wall, and the movements of the mouse were video-recorded for 10 min. Peanut butter chips were weighted before and after the test, and the "food zone" was defined as the area immediately surrounding the peanut butter chip (78 mm diameter, with the peanut butter chip at the center). Individual entries were defined as the mouse entering and then leaving the zone, with the length of the entry being defined as the amount of time the mouse was continuously tracked within that zone. Latency was defined as the time to approach one of the peanut butter chips after introduction into the open field.

The marble-burying test

The marble-burying test was conducted as described previously (*3*). Ten-week-old male mice were tested in either fed or fasted state. Mice were individually housed in a cage filled with 5 cm of novel bedding containing 24 × Ø 16-mm marbles evenly spaced across the bedding surface. Mice were then left undisturbed for the 30-min testing period. After 30 min, each mouse was returned to its home cage, and the number of marbles buried within the bedding was manually counted. Marbles buried <2/3 into the bedding were classified as not buried, and higher marble buried indicated a more pronounced obsessive-compulsive behavior.

Conditioned place preference

Fed or fasted mice had food removed for 1 hour to normalize satiety state before the test. The testing apparatus consisted of a rectangular cage constructed of plexiglass and contained three distinct side zones. The outer zones [28 cm (length) by 21 cm (width)] were differentiated by the wall pattern (full gray versus black and white strips) and the floor texture (soft versus rough), and a middle zone (21 cm by 9 cm) was separated from the other compartments by opaque white plexiglass walls. Mice were placed randomly into the apparatus, and a baseline preference of individual mice was evaluated. Mice spending between ≥45 and ≤55% on either side were considered to have no initial preference, and the most preferred side was paired with the chow pellets and the other with the peanut butter chips. For the conditioning, mice were exposed to either peanut butter chips or chow pellets alternately for 10 days with 20 min of exposure per session. The baseline preference and the trial day were video-recorded, and the time spent in the various compartment of the boxes was measured with the video-tracking software TopScan (CleverSys Inc., Reston, VA). For each conditioning session, food was removed 1 hour before baseline and trial sessions. On the trial day, neither chow nor peanut butter chips were available during the 20-min recording session. The preference score was calculated from the time spent in the specified conditioning compartment divided by the total time spent in both compartments, excluding the middle neutral zone, multiplied by 100.

Anhedonia test

Twelve-week-old male mice were randomly assigned and individually housed in cages with no bedding and access to two drinking bottles, one with water and one with artificial sweetener [0.1% (w/v) saccharin; Sigma-Aldrich, St. Louis, MO]. Mice were left undisturbed and allowed to drink ad libitum from either bottle for 48 hours. After 24 hours, the location of the two bottles was swapped to negate any potential confounding effects of place preference. Fluid intake from both bottles was measured every 24 hours for 2 days by weighing the bottles and subtracting the bottle weight.

Operant conditioning

Motivation was assessed using a nose-poke operant conditioning paradigm conducted with the Feeding Experimentation Device version 3 (FED3; https://hackaday.io/project/106885-feeding-experimentation-device-3-fed3). The FED3 consisted of active and inactive ports, with a nose poke on the active port producing light- and tone-conditioned stimuli, as well as a 20-mg sucrose pellet (TestDiet, St. Louis, MO). Nose pokes on the active and inactive ports as well as

pellet deliveries and collection times were logged. Nose pokes on the inactive port had no consequence. For animals to acquire the task, we performed a fixed-ratio (FR) schedule. During the FR acquisition, FED3s were placed in individual animal cages for 3 hours before lights off to avoid any effects of stress on task acquisition. FR1 equals one nose poke for one pellet; FR3 equals three nose pokes for one pellet; FR5 equals five nose pokes for one pellet. FR acquisition consisted of FR1 × 3 days, FR3 × 3 days, and FR5 × 3 days. To test motivation, we performed a progressive ratio (PR) in which the number of pokes required to receive a pellet progressively increased following a Richardson-Roberts schedule (1, 2, 4, 6, 9, 12, 15, 20, 25, 32, 40, 50, etc.). PR sessions were conducted overnight with access to food. Mice consumed chow during the FR acquisition and first PR session, after which they were switched to a high-fat diet for 5 days before a second PR session. During the first and second PR sessions, mice were exposed to two FR5 sessions to consolidate learning.

Sucrose or saccharin preference tests

Eight-week-old male mice were individually housed in BioDAQ cages with ad libitum access to standard chow and drinking water via two separate water bottles. During a 48-hour acclimation period, one bottle was filled with water while the other bottle remained empty. Once acclimated, the empty bottle was filled with either 10% (w/v) sucrose or 0.1% (w/v) saccharin in water. Mice were left undisturbed with ad libitum access to both water and either 10% (w/v) sucrose or 0.1% (w/v) saccharin solution. After 24 hours, the location of the two bottles was swapped to negate any potential confounding effects of place preference. Fluid intake was measured on subsequent days and grouped into 15-min time bins. Mice had ad libitum access to chow diet throughout the experiment.

Intra-ARC rAAV injections

Following procedures previously described in (*33*), 8-week-old male *Stat3*$^{fl/fl}$ mice were stereotaxically injected (~1×10^{12} to 8×10^{12} viral particles/ml) with rAVVs expressing CMV-driven Cre recombinase and eGFP (AAV-Cre-GFP; UNC Vector Core) or eGFP alone (AAV-GFP; UNC Vector Core) bilaterally into the ARC (coordinates, bregma: anterior-posterior, −1.40 mm; dorsal-ventral, −5.80 mm; lateral, ±0.20 mm, 100 nl per side). rAAVs were infused using a Neuros syringe (Hamilton, Reno, NV) at a rate of 10 nl/min. Following infusion, the ultrafine needle was left indwelling and undisturbed for a further 15 min before being slowly retracted from the brain parenchyma over a period of 2 min. Subsequent experiments were conducted 2 weeks after rAAV administration.

Statistical analysis

Statistical significance was determined by a one-way or two-way analysis of variance (ANOVA) with multiple comparisons or, where indicated, repeated measures or a paired Student's *t* test as appropriate. $P < 0.05$ was considered significant: $^{*}P < 0.05$, $^{**}P < 0.01$, and $^{***}P < 0.001$.

SUPPLEMENTARY MATERIALS

Supplementary material for this article is available at http://advances.sciencemag.org/cgi/content/full/7/9/eabf4100/DC1

View/request a protocol for this paper from *Bio-protocol*.

REFERENCES AND NOTES

1. K. Timper, J. C. Bruning, Hypothalamic circuits regulating appetite and energy homeostasis: Pathways to obesity. *Dis. Model. Mech.* **10**, 679–689 (2017).
2. G. T. Dodd, T. Tiganis, Insulin action in the brain: Roles in energy and glucose homeostasis. *J. Neuroendocrinol.* **29**, 10.1111/jne.12513, (2017).
3. M. O. Dietrich, M. R. Zimmer, J. Bober, T. L. Horvath, Hypothalamic Agrp neurons drive stereotypic behaviors beyond feeding. *Cell* **160**, 1222–1232 (2015).
4. M. J. Krashes, S. Koda, C. P. Ye, S. C. Rogan, A. C. Adams, D. S. Cusher, E. Maratos-Flier, B. L. Roth, B. B. Lowell, Rapid, reversible activation of AgRP neurons drives feeding behavior in mice. *J. Clin. Invest.* **121**, 1424–1428 (2011).
5. M. A. Cowley, J. L. Smart, M. Rubinstein, M. G. Cerdán, S. Diano, T. L. Horvath, R. D. Cone, M. J. Low, Leptin activates anorexigenic POMC neurons through a neural network in the arcuate nucleus. *Nature* **411**, 480–484 (2001).
6. D. Atasoy, J. N. Betley, H. H. Su, S. M. Sternson, Deconstruction of a neural circuit for hunger. *Nature* **488**, 172–177 (2012).
7. Y. Aponte, D. Atasoy, S. M. Sternson, AGRP neurons are sufficient to orchestrate feeding behavior rapidly and without training. *Nat. Neurosci.* **14**, 351–355 (2011).
8. J. N. Betley, Z. F. Cao, K. D. Ritola, S. M. Sternson, Parallel, redundant circuit organization for homeostatic control of feeding behavior. *Cell* **155**, 1337–1350 (2013).
9. Y. Chen, R. A. Essner, S. Kosar, O. H. Miller, Y. C. Lin, S. Mesgarzadeh, Z. A. Knight, Sustained NPY signaling enables AgRP neurons to drive feeding. *eLife* **8**, e46348 (2019).
10. L. Engstrom Ruud, M. M. A. Pereira, A. J. de Solis, H. Fenselau, J. C. Bruning, NPY mediates the rapid feeding and glucose metabolism regulatory functions of AgRP neurons. *Nat. Commun.* **11**, 442 (2020).
11. M. J. Krashes, B. P. Shah, S. Koda, B. B. Lowell, Rapid versus delayed stimulation of feeding by the endogenously released AgRP neuron mediators GABA, NPY, and AgRP. *Cell Metab.* **18**, 588–595 (2013).
12. S. Luquet, F. A. Perez, T. S. Hnasko, R. D. Palmiter, NPY/AgRP neurons are essential for feeding in adult mice but can be ablated in neonates. *Science* **310**, 683–685 (2005).
13. W. W. Pan, M. G. Myers Jr., Leptin and the maintenance of elevated body weight. *Nat. Rev. Neurosci.* **19**, 95–105 (2018).
14. Y. Zhang, R. Proenca, M. Maffei, M. Barone, L. Leopold, J. M. Friedman, Positional cloning of the mouse obese gene and its human homologue. *Nature* **372**, 425–432 (1994).
15. J. Xu, C. L. Bartolome, C. S. Low, X. Yi, C. H. Chien, P. Wang, D. Kong, Genetic identification of leptin neural circuits in energy and glucose homeostases. *Nature* **556**, 505–509 (2018).
16. I. S. Farooqi, S. O'Rahilly, Monogenic obesity in humans. *Annu. Rev. Med.* **56**, 443–458 (2005).
17. A. J. Sipols, D. G. Baskin, M. W. Schwartz, Effect of intracerebroventricular insulin infusion on diabetic hyperphagia and hypothalamic neuropeptide gene expression. *Diabetes* **44**, 147–151 (1995).
18. S. C. Woods, E. C. Lotter, L. D. McKay, D. Porte Jr., Chronic intracerebroventricular infusion of insulin reduces food intake and body weight of baboons. *Nature* **282**, 503–505 (1979).
19. C. Benedict, W. Kern, B. Schultes, J. Born, M. Hallschmid, Differential sensitivity of men and women to anorexigenic and memory-improving effects of intranasal insulin. *J. Clin. Endocrinol. Metab.* **93**, 1339–1344 (2008).
20. M. Hallschmid, S. Higgs, M. Thienel, V. Ott, H. Lehnert, Postprandial administration of intranasal insulin intensifies satiety and reduces intake of palatable snacks in women. *Diabetes* **61**, 782–789 (2012).
21. L. Jessen, D. J. Clegg, S. D. Bouman, Evaluation of the lack of anorectic effect of intracerebroventricular insulin in rats. *Am. J. Physiol. Regul. Integr. Comp. Physiol.* **298**, R43–R50 (2010).
22. G. T. Dodd, S. Decherf, K. Loh, S. E. Simonds, F. Wiede, E. Balland, T. L. Merry, H. Münzberg, Z. Y. Zhang, B. B. Kahn, B. G. Neel, K. K. Bence, Z. B. Andrews, M. A. Cowley, T. Tiganis, Leptin and insulin act on POMC neurons to promote the browning of white fat. *Cell* **160**, 88–104 (2015).
23. J. C. Bruning, D. Gautam, D. J. Burks, J. Gillette, M. Schubert, P. C. Orban, R. Klein, W. Krone, D. Müller-Wieland, C. R. Kahn, Role of brain insulin receptor in control of body weight and reproduction. *Science* **289**, 2122–2125 (2000).
24. A. C. Konner, R. Janoschek, L. Plum, S. D. Jordan, E. Rother, X. Ma, C. Xu, P. Enriori, B. Hampel, G. S. Barsh, C. R. Kahn, M. A. Cowley, F. M. Ashcroft, J. C. Brüning, Insulin action in AgRP-expressing neurons is required for suppression of hepatic glucose production. *Cell Metab.* **5**, 438–449 (2007).
25. M. P. Myers, J. N. Andersen, A. Cheng, M. L. Tremblay, C. M. Horvath, J. P. Parisien, A. Salmeen, D. Barford, N. K. Tonks, TYK2 and JAK2 are substrates of protein-tyrosine phosphatase 1B. *J. Biol. Chem.* **276**, 47771–47774 (2001).
26. S. Galic, M. Klingler-Hoffmann, M. T. Fodero-Tavoletti, M. A. Puryer, T. C. Meng, N. K. Tonks, T. Tiganis, Regulation of insulin receptor signaling by the protein tyrosine phosphatase TCPTP. *Mol. Cell. Biol.* **23**, 2096–2108 (2003).
27. G. T. Dodd, Z. B. Andrews, S. E. Simonds, N. J. Michael, M. De Veer, J. C. Brüning, D. Spanswick, M. A. Cowley, T. Tiganis, A hypothalamic phosphatase switch coordinates energy expenditure with feeding. *Cell Metab.* **26**, 375–393.e7 (2017).
28. E. Balland, W. Chen, G. T. Dodd, G. Conductier, R. Coppari, T. Tiganis, M. A. Cowley, Leptin signaling in the arcuate nucleus reduces insulin's capacity to suppress hepatic glucose production in obese mice. *Cell Rep.* **26**, 346–355.e3 (2019).

29. K. K. Bence, M. Delibegovic, B. Xue, C. Z. Gorgun, G. S. Hotamisligil, B. G. Neel, B. B. Kahn, Neuronal PTP1B regulates body weight, adiposity and leptin action. *Nat. Med.* **12**, 917–924 (2006).
30. G. T. Dodd, N. J. Michael, R. S. Lee-Young, S. P. Mangiafico, J. T. Pryor, A. C. Munder, S. E. Simonds, J. C. Brüning, Z. Y. Zhang, M. A. Cowley, S. Andrikopoulos, T. L. Horvath, D. Spanswick, T. Tiganis, Insulin regulates POMC neuronal plasticity to control glucose metabolism. *eLife* **7**, e38704 (2018).
31. W. A. Banks, J. B. Jaspan, A. J. Kastin, Selective, physiological transport of insulin across the blood-brain barrier: Novel demonstration by species-specific radioimmunoassays. *Peptides* **18**, 1257–1262 (1997).
32. G. T. Dodd, R. S. Lee-Young, J. C. Bruning, T. Tiganis, TCPTP regulates insulin signaling in AgRP neurons to coordinate glucose metabolism with feeding. *Diabetes* **67**, 1246–1257 (2018).
33. G. T. Dodd, C. E. Xirouchaki, M. Eramo, C. A. Mitchell, Z. B. Andrews, B. A. Henry, M. A. Cowley, T. Tiganis, Intranasal targeting of hypothalamic PTP1B and TCPTP reinstates leptin and insulin sensitivity and promotes weight loss in obesity. *Cell Rep.* **28**, 2905–2922.e5 (2019).
34. M. Elchebly, P. Payette, E. Michaliszyn, W. Cromlish, S. Collins, A. L. Loy, D. Normandin, A. Cheng, J. Himms-Hagen, C. C. Chan, C. Ramachandran, M. J. Gresser, M. L. Tremblay, B. P. Kennedy, Increased insulin sensitivity and obesity resistance in mice lacking the protein tyrosine phosphatase-1B gene. *Science* **283**, 1544–1548 (1999).
35. S. Galic, C. Hauser, B. B. Kahn, F. G. Haj, B. G. Neel, N. K. Tonks, T. Tiganis, Coordinated regulation of insulin signaling by the protein tyrosine phosphatases PTP1B and TCPTP. *Mol. Cell. Biol.* **25**, 819–829 (2005).
36. M. L. Piper, E. K. Unger, M. G. Myers Jr., A. W. Xu, Specific physiological roles for signal transducer and activator of transcription 3 in leptin receptor-expressing neurons. *Mol. Endocrinol.* **22**, 751–759 (2008).
37. S. M. Steculorum, J. Ruud, I. Karakasilioti, H. Backes, L. Engström Ruud, K. Timper, M. E. Hess, E. Tsaousidou, J. Mauer, M. C. Vogt, L. Paeger, S. Bremser, A. C. Klein, D. A. Morgan, P. Frommolt, P. T. Brinkkötter, P. Hammerschmidt, T. Benzing, K. Rahmouni, F. T. Wunderlich, P. Kloppenburg, J. C. Brüning, AgRP neurons control systemic insulin sensitivity via myostatin expression in brown adipose tissue. *Cell* **165**, 125–138 (2016).
38. D. Wang, X. He, Z. Zhao, Q. Feng, R. Lin, Y. Sun, T. Ding, F. Xu, M. Luo, C. Zhan, Whole-brain mapping of the direct inputs and axonal projections of POMC and AgRP neurons. *Front. Neuroanat.* **9**, 40 (2015).
39. M. O. Dietrich, J. Bober, J. G. Ferreira, L. A. Tellez, Y. S. Mineur, D. O. Souza, X. B. Gao, M. R. Picciotto, I. Araújo, Z. W. Liu, T. L. Horvath, AgRP neurons regulate development of dopamine neuronal plasticity and nonfood-associated behaviors. *Nat. Neurosci.* **15**, 1108–1110 (2012).
40. A. L. Alhadeff, N. Goldstein, O. Park, M. L. Klima, A. Vargas, J. N. Betley, Natural and drug rewards engage distinct pathways that converge on coordinated hypothalamic and reward circuits. *Neuron* **103**, 891–908 e6 (2019).
41. R. G. Denis, A. Joly-Amado, E. Webber, F. Langlet, M. Schaeffer, S. L. Padilla, C. Cansell, B. Dehouck, J. Castel, A.-S. Delbès, S. Martinez, A. Lacombe, C. Rouch, N. Kassis, J.-A. Fehrentz, J. Martinez, P. Verdié, T. S. Hnasko, R. D. Palmiter, M. J. Krashes, A. D. Güler, C. Magnan, S. Luquet, Palatability can drive feeding independent of AgRP neurons. *Cell Metab.* **22**, 646–657 (2015).
42. N. Turner, G. M. Kowalski, S. J. Leslie, S. Risis, C. Yang, R. S. Lee-Young, J. R. Babb, P. J. Meikle, G. I. Lancaster, D. C. Henstridge, P. J. White, E. W. Kraegen, A. Marette, G. J. Cooney, M. A. Febbraio, C. R. Bruce, Distinct patterns of tissue-specific lipid accumulation during the induction of insulin resistance in mice by high-fat feeding. *Diabetologia* **56**, 1638–1648 (2013).
43. E. D. Berglund, C. Y. Li, G. Poffenberger, J. E. Ayala, P. T. Fueger, S. E. Willis, M. M. Jewell, A. C. Powers, D. H. Wasserman, Glucose metabolism in vivo in four commonly used inbred mouse strains. *Diabetes* **57**, 1790–1799 (2008).
44. O. Fu, Y. Iwai, M. Narukawa, A. W. Ishikawa, K. K. Ishii, K. Murata, Y. Yoshimura, K. Touhara, T. Misaka, Y. Minokoshi, K. I. Nakajima, Hypothalamic neuronal circuits regulating hunger-induced taste modification. *Nat. Commun.* **10**, 4560 (2019).
45. K. Tan, Z. A. Knight, J. M. Friedman, Ablation of AgRP neurons impairs adaption to restricted feeding. *Mol. Metab.* **3**, 694–704 (2014).
46. E. van de Wall, R. Leshan, A. W. Xu, N. Balthasar, R. Coppari, S. M. Liu, Y. H. Jo, R. G. MacKenzie, D. B. Allison, N. J. Dun, J. Elmquist, B. B. Lowell, G. S. Barsh, C. de Luca, M. G. Myers Jr., G. J. Schwartz, S. C. Chua Jr., Collective and individual functions of leptin receptor modulated neurons controlling metabolism and ingestion. *Endocrinology* **149**, 1773–1785 (2008).
47. J. Mayer, Glucostatic mechanism of regulation of food intake. *N. Engl. J. Med.* **249**, 13–16 (1953).
48. K. J. Melanson, M. S. Westerterp-Plantenga, L. A. Campfield, W. H. Saris, Blood glucose and meal patterns in time-blinded males, after aspartame, carbohydrate, and fat consumption, in relation to sweetness perception. *Br. J. Nutr.* **82**, 437–446 (1999).
49. L. A. Campfield, F. J. Smith, Transient declines in blood glucose signal meal initiation. *Int. J. Obes. (Lond)* **14** (suppl 3), 15–31 (1990).
50. I. M. Chapman, E. A. Goble, G. A. Wittert, J. E. Morley, M. Horowitz, Effect of intravenous glucose and euglycemic insulin infusions on short-term appetite and food intake. *Am. J. Physiol.* **274**, R596–R603 (1998).
51. G. H. Anderson, D. Woodend, Consumption of sugars and the regulation of short-term satiety and food intake. *Am. J. Clin. Nutr.* **78**, 843S–849S (2003).
52. C. A. Campos, A. J. Bowen, M. W. Schwartz, R. D. Palmiter, Parabrachial CGRP neurons control meal termination. *Cell Metab.* **23**, 811–820 (2016).
53. R. A. Essner, A. G. Smith, A. A. Jamnik, A. R. Ryba, Z. D. Trutner, M. E. Carter, AgRP neurons can increase food intake during conditions of appetite suppression and inhibit anorexigenic parabrachial neurons. *J. Neurosci.* **37**, 8678–8687 (2017).
54. J. N. Betley, S. Xu, Z. F. H. Cao, R. Gong, C. J. Magnus, Y. Yu, S. M. Sternson, Neurons for hunger and thirst transmit a negative-valence teaching signal. *Nature* **521**, 180–185 (2015).
55. S. M. Sternson, D. Atasoy, J. N. Betley, F. E. Henry, S. Xu, An emerging technology framework for the neurobiology of appetite. *Cell Metab.* **23**, 234–253 (2016).
56. K. W. Williams, L. O. Margatho, C. E. Lee, M. Choi, S. Lee, M. M. Scott, C. F. Elias, J. K. Elmquist, Segregation of acute leptin and insulin effects in distinct populations of arcuate proopiomelanocortin neurons. *J. Neurosci.* **30**, 2472–2479 (2010).
57. J. W. Hill, C. F. Elias, M. Fukuda, K. W. Williams, E. D. Berglund, W. L. Holland, Y. R. Cho, J. C. Chuang, Y. Xu, M. Choi, D. Lauzon, C. E. Lee, R. Coppari, J. A. Richardson, J. M. Zigman, S. Chua, P. E. Scherer, B. B. Lowell, J. C. Brüning, J. K. Elmquist, Direct insulin and leptin action on pro-opiomelanocortin neurons is required for normal glucose homeostasis and fertility. *Cell Metab.* **11**, 286–297 (2010).
58. M. Grohmann, F. Wiede, G. T. Dodd, E. N. Gurzov, G. J. Ooi, T. Butt, A. A. Rasmiena, S. Kaur, T. Gulati, P. K. Goh, A. E. Treloar, S. Archer, W. A. Brown, M. Muller, M. J. Watt, O. Ohara, C. A. McLean, T. Tiganis, Obesity drives STAT-1-dependent NASH and STAT-3-dependent HCC. *Cell* **175**, 1289–1306.e20 (2018).
59. S. H. Lockie, C. V. McAuley, S. Rawlinson, N. Guiney, Z. B. Andrews, Food seeking in a risky environment: A method for evaluating risk and reward value in food seeking and consumption in mice. *Front. Neurosci.* **11**, 24 (2017).

Acknowledgments

Funding: This work was supported by the National Health and Medical Research Council (NHMRC) of Australia (to T.T. and Z.B.A.); T.T. and Z.B.A. are NHMRC Research Fellows. **Author contributions:** Conceptualization: T.T. and G.T.D. Methodology: T.T., G.T.D., S.J.K., M.M., C.E.X., J.C.B., and Z.B.A. Data acquisition: G.T.D., S.J.K., M.M., C.E.X., and Z.B.A. Data analysis: T.T., G.T.D., S.J.K., M.M., C.E.X., J.C.B., and Z.B.A. Data interpretation: T.T., G.T.D., S.J.K., M.M., C.E.X., J.C.B., and Z.B.A. Writing—original draft: T.T. Writing—review and editing: T.T., G.T.D., S.J.K., M.M., C.E.X., J.C.B., and Z.B.A. Funding acquisition: T.T. and Z.B.A. **Competing interests:** The authors declare that they have no competing interests. **Data and materials availability:** All data needed to evaluate the conclusions in the paper are present in the paper and/or the Supplementary Materials. Additional data related to this paper may be requested from the authors.

Submitted 24 October 2020
Accepted 14 January 2021
Published 26 February 2021
10.1126/sciadv.abf4100

Citation: G. T. Dodd, S. J. Kim, M. Méquinion, C. E. Xirouchaki, J. C. Brüning, Z. B. Andrews, T. Tiganis, Insulin signaling in AgRP neurons regulates meal size to limit glucose excursions and insulin resistance. *Sci. Adv.* **7**, eabf4100 (2021).